Max-Planck-Institut
für Meteorologie

REPORT No. 271

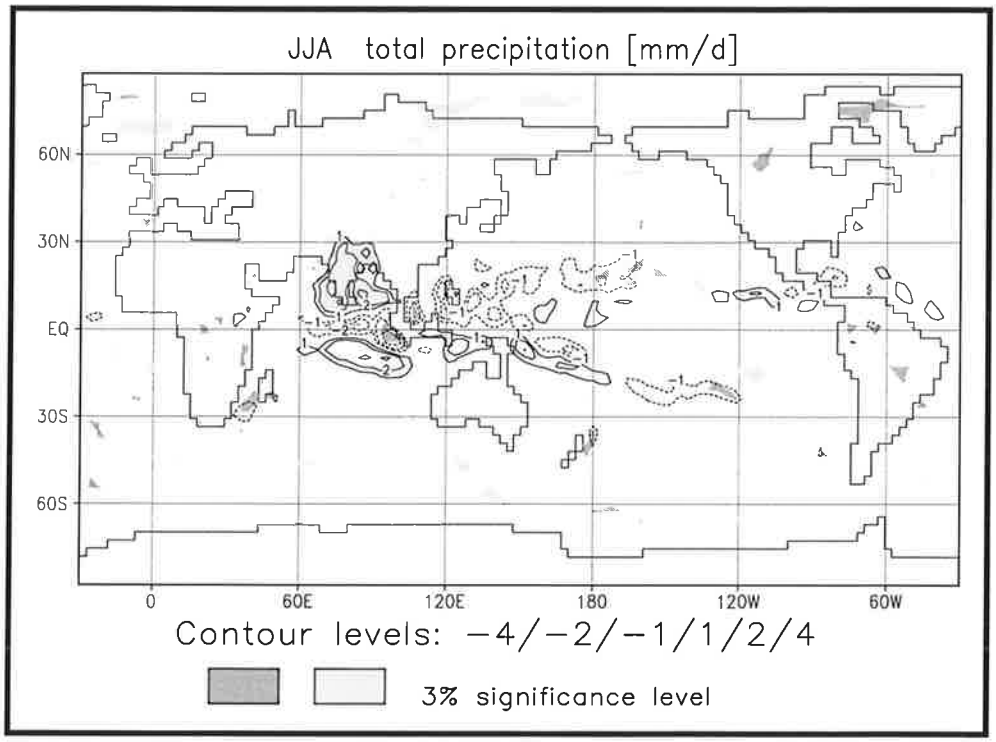

PORTRAYAL OF THE INDIAN SUMMER MONSOON IN THE LAND-OCEAN-ATMOSPHERE SYSTEM OF A COUPLED GCM

by

Lydia Dümenil

HAMBURG, August 1998

AUTHOR:

Lydia Dümenil

Max-Planck-Institut für Meteorologie
Hamburg
Germany

MAX-PLANCK-INSTITUT
FÜR METEOROLOGIE
BUNDESSTRASSE 55
D-20146 HAMBURG
F.R. GERMANY

Tel.: +49 - (0)40 - 411 73 - 0
Telefax: +49 - (0)40 - 411 73 - 298
E-Mail: <name>@dkrz.de

ISSN 0937 – 1060

Portrayal of the Indian summer monsoon in the land-ocean-atmosphere system of a coupled GCM

Lydia Dümenil

Max-Planck-Institut für Meteorologie
Bundesstr. 55
D-20146 Hamburg

ISSN 0937 - 1060

Abstract

A 150 year-long numerical simulation of present-day climate using the Max-Planck Institute's coupled ocean-atmosphere model ECHAM4-T42-OPYC3 is analysed with regard to the interannual variability of the strength of the Indian summer monsoon and its relation to land-surface and ocean interactions. Individual years are categorised into three classes of monsoons: normal, strong and weak (greater or less than one standard deviation of precipitation over India). The ensembles of anomalous monsoons are then sub-divided into a composite of cases coinciding with sea surface temperature (SST) anomalies in the Pacific related to the El Niño-Southern Oscillation (ENSO) phenomenon and a second composite of anomalous monsoons occurring, when no SST anomalies are found in the Pacific. The coupled model shows variations of the SST in the Pacific which are as large as and occur at a similar frequency as in observations. Thus it provides the basis for a realistic simulation of the interannual monsoon variability in ENSO-related conditions, but it overemphasizes the biennial component of occurrence. As in observations, about a third of all cases of weak monsoons occur in the summer when an El Niño begins to develop in the Pacific, while strong monsoons are often associated with La Niña events. This is an improvement from earlier coupled model simulations. In the model simulation, a modulation of the strength of the monsoon is due to a change of the large-scale land/ocean temperature gradient in the Indian Ocean sector in the mid-troposphere. The two composites show different developments during the annual cycle. In ENSO-related strong monsoon cases the atmosphere over land warms up during the spring in association with generally warmer tropics as a remnant from a warm event in the previous winter. During the summer months the warming in the Indian Ocean region is replaced by a cooling in association with the developing La Niña, while the land remains significantly warmer than normal. Therefore, in the coupled simulation the Indian Ocean only shows very small SST anomalies, while observed SSTs may vary in connection with ENSO events at a time lag of four months. Also for non-ENSO related monsoons a warming occurs over land in the summer, but then neither the Indian Ocean nor the tropical west Pacific exhibit any significant anomalies during the spring. Simulated temperature anomalies responsible for these modulations are relatively small. Independent of the origin of the monsoon anomaly, strong monsoons differ from weak monsoons by a significant precipitation pattern over India and a modification of the 850 hPa zonal wind field over the maritime continent and the West Pacific. Similar to observations, the anomalous monsoons in the coupled model are related to precursors in the 200 hPa zonal wind field in the spring, but no evidence could be found for a significant influence from the Eurasian snow pack in the spring on the subsequent Indian summer monsoon. While the model shows many realistic features, the variation of the monsoon occurs against a background of a deficient regional rainfall pattern in India and too small a range of Indian Ocean SST variations in conjunction with ENSO events.

1. Introduction

Contrary to most other parts of the globe, the meteorology of the South Asian region is dominated not by the sequence of daily weather but by a half-yearly change of the circulation (Normand, 1953). The most important atmospheric phenomenon in this region is the monsoon, which occurs at the height of the summer seasons in the Northern and Southern Hemispheres. The monsoon is considered a planetary feature affecting all major land masses where the differential heating between the oceans and the continents is the main driving force (Das, 1986). This study will focus on the summer monsoon in the vicinity of the Indian subcontinent.

In the Northern Hemisphere the winter-time dry north-easterly surface flow directed from the Asian continent to the ocean is regularly and abruptly replaced in June by a moist south-westerly flow from the ocean into the continent. The monsoon season ends with the so-called withdrawal of the monsoon in September. Although the monsoon occurs with remarkable regularity in the annual cycle in the tropics, it is subjected to an interannual variation in the dates of both the onset and withdrawal, i.e. the variation in the length of the monsoon season, as well as in the amount of rainfall during the season (Fig. 1). It is important to study the predictability of the anomalies in the rainfall over India because of their large socio-economic impacts, and those of the wind field associated with the monsoon due to their possible interaction with the ocean dynamics in the Pacific. Webster and Yang (1992) and Webster (1995) have indicated that the interaction between the global monsoon systems, and in particular the Indian monsoon, needs to be considered in order to improve the prediction of the El Niño-Southern Oscillation (ENSO) phenomenon as a part of the coupled land-ocean-atmosphere climate system.

Research on the predictability of the monsoon in India using the snow cover over Tibet as a predictor (Blanford, 1884) began at the end of the last century after the great famine in 1877. Since then many other predictors have been used to forecast the strength of the monsoon. Anomalies in the strength of the monsoon may have multiple causes. The regular occurrence of the half yearly reversal of the monsoon circulation in the annual cycle depends on the level of heating of the land masses (Das, 1986), i.e. the temperature gradient between land and ocean, and the presence of the Himalayan mountain range (Prell and Kutzbach, 1992). In particular, Flohn (1964) pointed out that the tropical easterly jet, which is characteristic of the tropical northern hemisphere summer circulation, is caused by a circulation from the warm land to the relatively cool Indian Ocean in the upper part of the troposphere. Therefore disturbed conditions over the continents may cause monsoon anomalies. On the other hand, the tropical convection is subjected to modulations of the Walker circulation in association with sea surface temperature (SST) anomalies in the Pacific. The predictability of the overall tropical circulation is therefore tied to that of the boundary conditions (Charney and Shukla, 1981), and the El Niño/Southern Oscillation phenomenon in the Pacific has been identified as a major player in the predictability of the monsoon (Palmer et al., 1992; Joseph et al., 1994). Many anomalous monsoons appear

in the summer when an ENSO event is developing in the Pacific, causing an eastward shift of the rising branch of the Walker circulation which in turn reduces the precipitation over India. Sea surface temperature anomalies in the eastern Pacific (Rasmussen and Carpenter, 1983) have thus been suggested as potential predictors for Indian monsoon rainfall.

Shukla and Paolino (1983) noted that Indian rainfall anomalies were highly correlated with an index of the Southern Oscillation in the autumn and winter following the monsoon season, while Yasunari (1990) and Webster and Yang (1992) found that the lag-correlation between Indian monsoon rainfall and equatorial Pacific sea surface temperature was small in the winter previous to the monsoon and slowly grows during the actual monsoon season to reach values of 60% in the autumn and winter after the monsoon. These two studies were based on relatively short time series of about 15 years. The analysis of ninety years of observations showed that the strength of this lag-correlation is different in the earlier parts of this century than in the decade of the 1980s (Arpe et al., 1998). Meehl (1994) suggested that cold tropical Indian Ocean SSTs during the winter season preceding the monsoon may be responsible for deficient monsoon precipitation over India, and correlations between all-India rainfall and observed SSTs for the period 1979-1994 indicate that highest correlations are indeed found in the Arabian Sea (Arpe et al., 1998). Long time series of precipitation over the Indian subcontinent are available from 1871 onwards (Sontakke et al., 1993), but the observational data coverage for the atmosphere and oceans in general has only been good enough for quantitative studies during the last twenty years. So far, neither observations nor modelling studies have been able to present a coherent picture of all the processes and interactions which are currently being discussed.

The weak and strong monsoon cases of 1987 and 1988 were studied by a set of numerical experiments coordinated by the Tropical Ocean Global Atmosphere (TOGA) Monsoon Numerical Experimentation Group (MONEG) (Palmer et al., 1992; Dümenil and Roeckner, 1992; WMO, 1993; Arpe et al., 1998) in a search for the relative influence of the initial conditions and boundary conditions such as the Pacific ENSO and the Indian Ocean sea surface temperature anomalies and soil moisture conditions over the continents.

In the context of the coupled land-ocean-atmosphere system, the reanalyses of the National Center for Environmental Prediction (NCEP; Kalnay et al., 1996) and the European Centre for Medium-Range Weather Forecasts (ECMWF; Gibson et al., 1997), give a good general representation of the climatology of the tropical easterly jet and the precipitation and convection in South Asia (Dümenil and Bauer, 1998). During the period 1979-1993 covered by the reanalyses the year 1979 is the only case of a significantly anomalous monsoon that does not coincide with an SST anomaly in the Pacific. The MONEG results lead to the impression that strong monsoons were synonymous with La Niña events and weak monsoons with El Niño events (Ju and Slingo, 1995). The case of 1979, however, points to an influence from other sources, because the monsoon is anomalous while there is no Pacific SST anomaly. More

recently, in 1997, a strong Pacific SST anomaly was associated with a normal monsoon over India while SSTs in the Indian Ocean deviated from the normal conditions. Yasunari et al. (1991) suggested that the chaotic dynamics of the mid-latitudes may contribute to large-scale anomalies at the land surface over Eurasia reflected in the snow, soil moisture and land surface temperature fields, and would subsequently result in a variation of the strength of the monsoon. In particular anomalies in the winter and early spring snow pack over the Himalayas (Blanford, 1884) or on the large-scale over Eurasia (Hahn and Shukla, 1976; Dickson, 1984; Khandekar, 1991; Sankar-Rao et al., 1996) have been related to the strength of the subsequent Indian summer rainfall.

The snow cover exerts a direct radiative effect on the surface energy budget, but the land surface also provides the memory through which a larger amount of snow increases the soil moisture and leaves the land surface cooler than normal well into the spring. As a consequence, the north-south temperature gradient, which is responsible for the reversal of the monsoon circulation, is reduced. This physical mechanism has been successfully reproduced in model studies (Barnett et al., 1989; Vernekar et al., 1995; Douville and Royer, 1996). In an observational study, Yang (1996) relates Eurasian snow cover extent to Indian summer monsoon rainfall and confirms the inverse relationship between these parameters. However, this relationship is disrupted during El Niño winters, when the extent of the Eurasian snow line is larger than normal. Due to the current lack of suitable data, the study of the interannual variability of the snow depth (water equivalent) in Eurasia is difficult. Corti et al. (1998), however, find a significant relationship between the positive/negative phase of the snow depth anomaly and warm/cold ENSO events for ensembles of ECMWF winter seasonal forecasts.

A large ensemble of cases is required to separate the effects due to the land and the SST, but even the reanalyses do not provide a large enough sample. In addition, there is no good observational database for any of the surface fields such as snow and soil moisture that would be consistent with atmospheric fields.

Alternatively, results from long integrations using coupled atmosphere-ocean general circulation models (CGCMs) may be used to study the processes involved. Such models provide a full description in space and time of the atmosphere and ocean for a plethora of variables, and are a unique tool to study interactions and sensitivities. It has to be determined, however, if CGCMs represent all or only some of the processes that are instrumental in establishing the observed level of variability of the tropical circulation. Until recently, coupled model simulations have shown errors in the magnitude and frequency of SST anomalies in the equatorial Pacific and Indian Ocean so that an interaction between the monsoon and the oceans could not be satisfactorily studied (Latif et al., 1994). The same applied to the rather rudimentary treatment of land surface hydrology. However, the CGCM of the Max-Planck Institute (MPI) which will be used in this study shows ENSO events of about the same magnitude and frequency as the

observations, and their teleconnections were found to be realistically simulated in North America and Europe (Roeckner et al., 1996a, May and Bengtsson, 1996). Moreover, the hydrological cycle over land is by and large also well represented by the atmospheric part of the model (Hagemann and Dümenil, 1998).

In the present paper we shall take the debate on model simulated interannual variability one step further by taking the land surface processes into account. We shall study the performance of a 150 year simulation using the coupled ECHAM4-T42-OPYC3 model (Roeckner et al., 1996a) with regard to aspects of interannual variability in South Asia, related to both the land and the oceans. The emphasis will be on documenting the hypothesis that both continental and oceanic temperature and circulation anomalies may have an influence on the strength of the monsoon and how they are represented by the model. The long coupled model simulation can provide a sufficient sample of strong and weak monsoons from which a difference between ENSO-related and non-ENSO-related monsoon anomalies can be established. This is an important requirement because the continental parameters influencing the monsoon can only be studied if there is no major influence from SST anomalies in the Pacific at the same time.

The model and its relevant climatology are described in Section 2. Section 3 describes how the 150 year integration is sub-divided into composites. Differences between ENSO-related and non-ENSO-related monsoon composites are discussed in Section 4. Results are summarized in Section 5.

2. Description of the Model and its Climatology

2.1. The Coupled Ocean-Atmosphere Model

The ECHAM4-OPYC3 coupled ocean-atmosphere general circulation model (Roeckner et al., 1996a) was integrated for several hundred years in a simulation of present-day climate. From this simulation, a sequence of 150 model years was available for analysis in this study. The model consists of the atmospheric model ECHAM4 at T42 resolution (Roeckner et al., 1996b) and the isopycnal ocean model OPYC3 (Oberhuber, 1993) comprising a deep ocean, a mixed layer and a sea-ice model. The two models are coupled via an exchange of freshwater and turbulent fluxes of heat and momentum. The flux adjustment which is used in order to minimize the drift of the coupled model is only applied to the annual mean values of turbulent heat and freshwater fluxes; wind stress is not flux-adjusted.

2.2. The Variability of the Sea Surface Temperature

The model shows a high degree of skill in representing the climatology and interannual variability of the atmospheric and oceanic circulations. The time sequence of NINO3 (5S-5N, 150W-90W) SSTs is shown in Fig. 2. In general, the horizontal patterns of SSTs deviate from

observations by only up to 1 K, with largest errors occurring in the region of the boundary currents for which the resolution of the model (2.8°, increasing to 0.5° from 36°N/S to the equator) is not sufficient (Roeckner et al., 1996a). In comparison to the Global Ice and Sea Surface Temperature (GISST) dataset (Rayner et al., 1996) for the period 1949-91, the model shows a realistic interannual variability (Roeckner et al., 1996a). This MPI model is capable of simulating ENSO-related events in the tropical ocean of similar frequency of occurrence and magnitude as observed. The frequency of El Niño events in the model is about 4 years which agrees well with the observed frequency of 3.8 years found by Quinn et al. (1987). The biennial component in the model events is, however, stronger than in the observations. Simulated El Niño events also display a decadal variability ranging from 3 K events similar to that observed in 1982-83 to smaller ones of just under 1 K. Following Roeckner et al. (1996a), SST anomalies are classified as ENSO events if they are greater than 1 K in amplitude and persist for more than one year. In Fig. 2 such events are marked by solid bars.

The model simulated ENSO events are tied to the annual cycle in a realistic way, with maxima in the northern hemisphere winter (Torrence and Webster, 1995), but with the transition between warm and cold ENSO phases in the spring being too abrupt (Roeckner et al., 1996a). From the point of view of representation of the ocean, the model has state-of-the-art accuracy and seems to be a useful tool to study the relationship between ENSO events and the monsoon.

2.3 The Climatology of Composite El Niño Events

From the 150 year model simulation we chose 32 El Niño events, whose average time evolution is given in Fig. 3. At the height of their development, all El Niño cases show maximum temperatures which are similar to those observed during the 1980s. Although the SSTs of the decade of the 1980s are not representative of El Niño development in general, they are used here to document the SSTs which were observed (Reynolds and Smith, 1994) during the period for which a number of atmospheric fields are available in assimilated form through the reanalysis, and are therefore the SSTs that are most consistent with the atmospheric fields. The ECMWF reanalysis is used to validate the atmospheric fields of the coupled integration. For further comparison, the corresponding evolution is also displayed for the GISST dataset (Rayner et al., 1996) in Fig. 3.

A major disagreement is found in the fact that the model exhibits a much stronger biennial variation in NINO3 SSTs than is observed, and this is also reflected in the atmospheric response. The model results describe a typical biennial sequence centred on a mature northern hemisphere wintertime El Niño with a high likelihood of a La Niña event in both the preceding and following boreal winters. Neither the average of the El Niños occurring during the reanalysis period (1982-83, 1986-87, 1991-92) nor the averaged GISST annual cycle support this feature (Fig. 3). The maxima of model simulated SST have a tendency to occur in

November instead of December. As the SST levels of the preceding winters are therefore generally too low, the transition in the spring is too fast. The same applies to the decay in the late winter and spring of the following year. Although the averages of the two ensembles agree, the range of interannual variations is larger in late winter for the ECMWF reanalysis and larger in the summer in the model simulation. Note that the observed SST ensemble (Reynolds and Smith, 1994) contains only three ENSO events, while the model simulation ensemble contains 32 cases.

With respect to the evolution of SST anomalies in the NINO3 area in the late spring and early summer at the time of the onset of the monsoon, the model agrees better with the SSTs of the 1980s than with the long-term averaged GISST (Fig.3). In the summer, GISST data show a smaller value of SST anomalies than the observations by Reynolds and Smith (1994).

At the maturity of the El Niño event, the center of convection shifts eastward as observed (not shown). Both the model and the reanalysis agree on the reduction of precipitation over the land in India in the summer while the El Niño is developing. The resemblance of the model's response to the reanalysis is, however, much less in the equatorial Indian Ocean region and outside the tropics. While the typical atmospheric ENSO response during the period covered by the reanalysis shows a relatively large-scale precipitation anomaly developing over the Indian Ocean in the summer when SSTs begin to rise, the model simulates a shift of the convection only in a relatively narrow band along the equator.

The model-simulated precipitation anomalies (not shown) are significant over India and the Pacific Ocean region during the whole year starting in March/April/May of a year leading up to a mature El Niño, but the anomalies of the summer monsoon precipitation over India in the year following the mature El Niño are not significant.

The anomalies of the precipitation field are consistent with the global-scale anomalies as, for example, seen in the 200 hPa velocity potential (not shown). While the ECMWF reanalysis shows dipole anomalies in the velocity potential for El Niño cases all year round, the model simulated anomalies are small in the spring because of the transition from La Niña to El Niño conditions (or vice versa). The model simulated sequence of precipitation anomalies during La Niña conditions is opposite in sign but of the same strength as those found during El Niño.

2.4. The Climatology of the Monsoon

The atmospheric component of the CGCM represents the monsoon climatology in the same way as the atmospheric model ECHAM4. Dümenil and Bauer (1998) compare the summertime tropical easterly jet at 200 hPa from different model versions and at different model resolutions, and find good agreement with the reanalyses everywhere with the exception of the entrance region of the tropical easterly jet. The correct positioning and strength of the jet depends on the

choice of the parameterisation schemes for convection and land surface processes as well as on the model's horizontal resolution. Only model versions that allow for a land surface which is as warm as observed can establish a strong heat low over the continent in the summer and therefore lead to a monsoon circulation which is as strong as that observed. The model version ECHAM4 at T42 resolution has a cold bias over Tibet and overestimates convection in the equatorial Indian Ocean so that the core velocity of the jet is slightly reduced and a secondary maximum appears near the equator.

Fig. 4 shows the precipitation field averaged over the summer season (June/July/August) for the ECMWF reanalysis, a climatology (Rudolf et al., 1992) and the 150-year coupled integration. Compared to the reanalysis and the climatology, the model puts too much emphasis on the convection in the Indian Ocean equatorial region, while the precipitation over the land in India is smaller than observed.

2.5. The Interannual Variability of the Monsoon

The problem of horizontal resolution is important when the traditional land-based observational datasets (Sontakke et al., 1993) for variability of monsoon precipitation are compared to model output. Webster and Yang (1992) pointed out that the wind shear between 850 and 200 hPa over the region of (40-110E, 0-20N) provides a good measure of the large-scale convective aspects of monsoon variability over India and the adjacent ocean, which to some extent appear in association with the NINO3 SST anomalies (Fig. 5a). Many large-scale GCMs can successfully represent the influence of the ENSO signal on the large-scale monsoon index. This also applies to the present model (Fig. 5b) which shows a higher correlation between the Webster-Yang index and the NINO3 SST than the ECMWF reanalysis. The time evolution of the large-scale monsoon index is, however, not very tightly correlated with the regional monsoon precipitation variability over land as described by the all-India rainfall (Parthasarathy et al., 1994) or the precipitation over corresponding land points in the ECMWF reanalyses (Fig. 6a). Ju and Slingo (1995) showed that their GCM provided a good representation of the variability of the monsoon index, but not of the regional all-India rainfall at land-based stations. Sperber and Palmer (1997) extended this diagnostic to all models participating in AMIP (Atmospheric Model Intercomparison Project; Gates, 1992) and found that half of the GCMs did not pass a quality test concerning the variation of the all-India rainfall as a response to the Pacific SST anomalies in 1987 and 1988. They found the models' skill in representing the monsoon variability in the tropics with respect to ENSO conditions to be highly sensitive to the horizontal resolution, and classified the results with respect to the formulation of the closure applied in the convection schemes. Dümenil and Bauer (1998) also found that the rainfall representation in the ECHAM model hierarchy is related to aspects of the parameterization of convection and land surface processes as well as horizontal resolution.

The ECHAM4-T42 model systematically underestimates the climatological mean rainfall and the interannual variability as compared to station observations which are only available over land in India. The monsoon rainfall, however, extends also over the adjacent oceans and eastward across the Bay of Bengal. As the reanalysis provides data over land as well as over the oceans, it is proposed to use a different measure of the seasonal monsoon rainfall in this study and to validate it against the ECMWF reanalysis. A small extension of the region of the test used by Sperber and Palmer (1997) (to cover 70-100E, 10-25N) is sufficient to coincide with the area where the Webster and Yang index correlates best with the local rainfall in the ECMWF reanalysis and also in the model (not shown). This reconciles the large-scale variation of the monsoon as measured by the Webster and Yang index with the local rainfall variation observed at the land stations over India (Fig. 6b). The ECHAM4-T42 atmosphere model represents this variability to an acceptable degree if it is forced by observed SSTs, although the amplitudes are smaller than most of the observed estimates covering the reanalysis period. Using the same criterion, the interannual variability of the Indian monsoon in the coupled model simulation analysed here (ECHAM4-OPYC3) is well captured (Fig. 2).

3. Composites of Strong and Weak Monsoons

In the following the standard deviation of the precipitation averaged over the area 70-100E and 10-25N and averaged over the entire monsoon season from June to September will be used to classify strong and weak monsoons. This criterion relates well to the large-scale aspects of the monsoon which are the only ones we can study given the present model resolution. Monsoons that deviate from the normal precipitation value (850 mm) by one standard deviation (84 mm) are very likely to lead to serious drought or flood situations in India. In Fig. 2 a standard deviation larger than +1 defines a strong monsoon, a value smaller than -1 indicates a weak monsoon. Years with extreme values during the 150 year record are indicated by thin bars in Fig. 2. The range of simulated anomalies is similar to that in the reanalysis (Fig. 1). In the 150 years of the simulation a total of 31 strong and 30 weak monsoon cases appeared. This frequency of occurrence of anomalies agrees well with observations from 1871 to 1991 (Mooley and Shukla, 1987, Kripalani, 1996).

Although there are 33 cases of El Niño and 32 cases of La Niña conditions in the NINO3 area in the simulation, the monsoon and ENSO anomalies do not, of course, coincide. The model quite realistically places most of the cases of anomalously strong monsoons in the northern hemisphere summer when a La Niña anomaly is developing. The weak monsoon anomalies are found in the summers that are followed by an El Niño event which reaches maturity during the following November. In very good agreement with observations (Mooley and Shukla, 1987), the model simulated strong monsoons are more likely to be followed by a La Niña event (15 cases) than to be followed by an El Niño event (2 cases). A strong monsoon is preceded by a La

Niña anomaly in only one case, while it is preceded by an El Niño in seven cases. A similar distribution but with opposite signs exists for weak monsoons. This leaves a relatively large sample of 19 cases of non-ENSO monsoon anomalies when the monsoon is anomalously strong and SST anomalies in the Pacific are very weak (Fig. 3). In the following, composites of strong and weak monsoons will be used to discuss the significantly distinctive features of the non-ENSO and the ENSO ensembles. Accordingly, three sets of composites were made:

a) all cases of strong and weak monsoons that occurred during the 150 years,

b) the ENSO monsoon ensemble consisting of all strong monsoons occurring during the summers leading up to a mature La Niña event and all weak monsoons occurring previous to a mature El Niño event,

c) the non-ENSO monsoon ensemble consisting of all strong and weak monsoons occurring when SST anomalies in the NINO3 region are near zero.

Fig. 3 compares the development of the typical simulated El Niño to the average El Niño of the 1980s. For comparison, Fig. 3 also describes the evolution of SST anomalies during an annual cycle when there are no ENSO events. This is the basis for the non-ENSO monsoon ensemble.

For several variables associated with the monsoon, seasonal averages (preceding winter, preceding spring, summer, autumn) were computed for these composites in order to describe the monsoon season itself, its development stage and the post-monsoon stage. The sizes of the ensembles and the length of the available integration ensure the significance of the anomalies. The differences between all strong and weak monsoons (not shown) are dominated by highly significant large-scale patterns of anomalies in all monsoon-related atmospheric variables which arise from the ENSO-related cases in the sample. As discussed above, their features agree well with the ECMWF reanalysis (which is dominated by ENSO-related cases). The ENSO ensemble is very similar to the cases of 1987 and 1988 which were studied in the MONEG experiments (Dümenil and Roeckner, 1992: Palmer et al., 1992; WMO, 1993; Arpe et al., 1998).

4. The Difference Between the ENSO- and the non-ENSO-Ensemble

4.1 The Monsoon Season

4.1.1 Precipitation

As expected, the precipitation (Fig. 7a) differences in the ENSO-monsoon ensemble between strong monsoons occurring during the summer of an El Niño (-1) year and weak monsoons

occurring in the summer of a La Niña (-1) year are significant (at the 97% level in a Student's t-test) in the Indian sector. Differences occur over the whole region of India and the adjacent oceans, with maxima placed off the coast by the Ghats mountain range, in the southern Bay of Bengal and in northern India. This behaviour is similar to the differences given by the ECMWF reanalysis (not shown). (Note that in the analysed ensemble all cases of extreme monsoons with the exception of 1979 are influenced by ENSO, and include the response to the very strong 1982-83 event.) But these anomalies are only a small part of the significant large-scale anomalies in the precipitation field which cover a large part of the globe. While the significant anomaly over the Indian peninsula exists only in June/July/August (JJA), the precipitation anomalies in the Pacific are widespread in the seasons preceding and following the monsoon as well. Precipitation anomalies along the equator in the Pacific are closely tied to the evolution of the SST anomalies leading up to the maximum ENSO anomaly in the following late autumn and winter. Due to the too strong biennial characteristics of the coupled integration, the patterns of precipitation anomalies in the Pacific in the winter preceding the monsoon (DJF) are reversed due to an ENSO state of opposite sign.

In the non-ENSO monsoon ensemble of ten cases of very small NINO3 SST anomalies (Fig. 3c), the only significant anomalies in the precipitation field (Fig. 7b) are those over the Indian subcontinent and the equatorial Indian Ocean, and they are restricted to the summer season. The magnitude of the precipitation anomaly in the Indian region and the position of the local maxima are very similar to that of the ENSO-monsoons. This regional pattern therefore defines the typical difference between strong and weak monsoons regardless of the origin of the variation. In contrast to the ENSO-monsoons, however, there are only a few scattered anomalies in the precipitation field over the Pacific which have a less coherent, almost noisy structure and are not significant.

4.1.2 Upper Air Fields

The variation of the monsoon in both the ENSO-ensemble and the non-ENSO-related monsoons is consistent with a significant difference in the strength of the upper air wind field (Fig. 8). In JJA both ensembles a considerable (significant) change of the subtropical jet is found in Eurasia and also, more pronounced, in the Southern Hemisphere. The most striking feature at the 200 hPa level is the strong widespread significant anomaly in the exit region of the tropical easterly jet and in equatorial and southern Africa. Again, this is a characteristic of both, ENSO- and non-ENSO related monsoons. In the ENSO-ensemble there are additional anomalies of global extent.

The precipitation anomaly of the non-ENSO monsoon anomalies in the region of the Indian Ocean is consistent with a large-scale anomaly of the velocity potential at 200 hPa (not shown), although this is much smaller (though still significant) than in the case of the ENSO-monsoons.

4.1.3 Atmospheric Temperature

In JJA at 500 hPa (Fig. 9), both the ENSO and the non-ENSO ensemble show a significant warming at 30 degrees latitude in the Northern and Southern Hemispheres in association with a small-scale cooling in the Indian Ocean region. The magnitude of the anomaly extending northward of 15°N over land is about 1 K at the maximum and is well in the range of anomalies which were applied in model sensitivity experiments investigating the influence from the land surface on the strength of the monsoon (Barnett et al., 1989; Vernekar et al., 1995; Douville and Royer, 1996). In the ENSO ensemble a cold anomaly has replaced the warm anomaly in the eastern tropical Pacific and now covers almost all of the tropical Pacific. The corresponding cooling in the Indian Ocean region is significant but very small. There are numerous other significant anomalies all over the globe in this situation, which develop into the well-known ENSO teleconnection patterns later in the year (SON). The typical difference between strong and weak monsoons in the JJA season in the model simulation therefore involves a warming over land and a very small cooling of the equatorial Indian Ocean. This cooling occurs during the switch from positive to negative anomalies during the too abrupt transition in SSTs in the spring and early summer in association with the strongly biennial variation of SSTs in the model.

The Indian Ocean region surface temperature (not shown) shows several regions of temperature anomalies during the JJA season in the ENSO cases associated with differences between strong and weak monsoons. The warm surface temperature anomaly extends over the land as well as parts of the Arabian Sea. In both the GISST (Rayner et al., 1996) and the Reynolds and Smith (1994) datasets the average range of the annual cycle of large-scale averaged (5S-20N, 50E-100E) SSTs in the Indian Ocean is less than ± 0.25 K. The variation is, however, such that occasionally, after an El Nino event, Indian Ocean temperature anomalies may reach values of 0.5 K. Venzke et al. (1997) discuss that this occurs at a time-lag of four months after the mature ENSO events in both the GISST observations and to a lesser degree in their model simulation. In comparison to this, during the reanalysis period, SSTs in this region show a slightly delayed average warm anomaly of about 0.5 K during the spring before the average strong monsoons. In the ENSO ensemble we find consistent variations of half the magnitude of the observed and no variation in the non-ENSO ensemble. The time evolution of Indian Ocean SST is, however, critical in the development of the temperature gradient between the land and the Indian Ocean. The reduced interannual variability may therefore lead to serious systematic errors by reducing one component of the interannual variability and will require further investigation.

4.1.4 The Near-Surface Wind Field

A strikingly similar anomaly pattern of the JJA 850 hPa wind field (Fig. 10) distinguishes years of extreme monsoons from normal years. Regardless of the presence of an ENSO signal or none in the Pacific, extreme monsoons show a pattern of lower troposheric wind anomalies in the region of the Somali jet, parts of Africa, the southern flanks of the Himalayas, the Bay of Bengal and the West Pacific north of the equator. The anomaly is consistent with the strength of the monsoon circulation in the Arabian Sea and may lead to upwelling in that region. Meehl (1987) and Yasunari (1990) suggested that stronger (weaker) than normal Indian monsoons are most probably followed by stronger (weaker) easterlies over the central Pacific which may trigger ENSO events. Model sensitivity studies (Barnett et al., 1989) lead to similar results. In the ENSO-ensemble, the West Pacific anomaly appears already in the preceding spring. It continues through the summer into the SON season, but migrates to the east. The non-ENSO cases (Fig. 10b) do not show this feature, with only a small anomaly remaining at the equator in SON.

4.2. The Preceding Spring

4.2.1 Upper Air Fields

In the search for a suitable precursor of the monsoon which may be exploited for prediction, it is useful to explore the set of variables associated with elements of the monsoon for ENSO-monsoons and non-ENSO-monsoons in terms of their behaviour during the spring preceding a strong or weak monsoon. Webster and Yang (1992) found a weakening of the subtropical jet in the spring preceding strong monsoons in the NMC (National Meteorological Center) analyses. Such anomalies also exist in the difference fields between the strong and weak monsoon cases in the ECMWF reanalysis (not shown). Yang et al. (1996) present evidence that such precursors can be successfully represented in atmospheric model simulations. Indeed in our simulation anomalies of similar strength occur in the zonal wind field at 200 hPa at various locations in both ensembles. In the non-ENSO monsoon composite (Fig. 8b) there are positive (significant at the 95% level) anomalies, i.e. a strengthening of the subtropical jet, in the region north of 30N in the Mediterranean region and in East Asia just to the north of the negative anomalies. At these locations we also find positive (but not significant) anomalies in the ENSO-ensemble. In addition, the ENSO-ensemble shows large-scale anomalies all over the Pacific. The strongest (significant) anomalies (a strengthening of the easterly jet in the strong monsoon case) in MAM are found in the entrance and exit regions of the tropical easterly jet, i.e. in the West Pacific, in the China Sea, and over Arabia and the Arabian Sea along 10N. Those in the West Pacific appear in conjunction with a local anomaly of the SST.

4.2.2 Atmospheric Temperature

In the spring, the ensemble of ENSO-monsoons shows a small but significant (at the 97% level) large-scale temperature anomaly at 500 hPa in the tropics (Fig. 9a) that distinguishes strong from weak monsoons. It covers almost all of the tropics and for strong monsoons it is associated with the general warming due to the El Niño event of the previous winter (DJF). The variation of Pacific SST in the model shows highly biennial characteristics, with a strong monsoon often occuring in the summer when a La Niña SST anomaly is developing (JJA and SON) and often being preceded by an El Niño (DJF). The spring is therefore often the season of transition from one event to one of the opposite sign.

In MAM the maximum of the warm anomaly is centered along 30°N over land. This is a significant anomaly and is in agreement with the difference between strong and weak monsoons in the ECMWF reanalysis (Fig. 9c). While in the ENSO-ensemble in MAM the tropics are warmer than usual over the ocean as well as over the continent in the case of a strong monsoon, the middle tropospheric temperatures over the continent are slightly warmer than over the adjacent Indian Ocean. This increases the temperature contrast that is responsible for setting up the monsoon circulation in the annual cycle. In parallel, the cold anomaly developing in the Pacific prevents the center of convection from moving eastward and therefore adds to the strength of the monsoon.

In the non-ENSO case, strong monsoons are distinguished from weak monsoons by a stronger land-ocean temperature contrast as well, but the development during the annual cycle is different. Here, the temperature in the Pacific Ocean region varies little during the annual cycle and in particular there is no reversal of sign from spring to summer as in the ENSO cases. In the spring, a small region of the West Pacific and parts of the equatorial Indian Ocean and the maritime continent (not significant) are cooler in the strong than in the weak cases, but absolute values are very small. The positioning of the anomalous heating in the model in the West Pacific agrees with the position of the high correlations between SST and all-India rainfall in the correlations of Arpe et al. (1998) during the months of JJA.

There is no anomaly over land in the spring (MAM). However, when the land warms up during the annual cycle, a warm anomaly develops in Arabia and northwest India extending into the northern parts of the Arabian Sea in JJA. A warming over the Arabian Sea at the beginning of the monsoon season is beneficial to the development of a stronger monsoon rainfall, because evaporation over the sea is enhanced and more humidity becomes available for precipitation (Mooley and Shukla, 1987; Arpe et al., 1998). (During the course of the monsoon season, the enhanced surface flow in the strong monsoon case is expected to cool the Arabian Sea through increased upwelling). In the observed SSTs (consistent with the reanalyses) the behaviour is similar, as the Bay of Bengal is the first to warm up in the spring followed by a warming of the

Arabian Sea in JJA. In JJA the cooling in the West Pacific spreads and becomes significant over a small region, thereby enhancing the land-sea heat contrast from which a stronger monsoon can develop.

In the case of the non-ENSO-monsoons there is no significant 500 hPa temperature anomaly over land in the spring. In the case of the ENSO-monsoons the temperature anomaly at 500 hPa over land south of 40°N between Egypt and China is associated with a shift of the subtropical jet in MAM. This agrees well with the preferred location of anomalies resulting from ENSO events in the ECHAM model. This region may be influenced by the chaotic atmospheric processes of the mid-latitudes which in turn may be modulated by disturbances induced by variations of Pacific SSTs. For the atmospheric part of the present CGCM the skill in representing teleconnections from ENSO events has been studied by Bengtsson et al. (1996) for integrations using prescribed interannually varying observed and climatological global SSTs from the AMIP period. These authors find that the observed variability in mid-latitudes is fully represented if climatological SSTs are used.

4.2.3. Representation of Atmospheric Teleconnections

The influence from the land in Eurasia on the monsoon in the coupled model is reflected by more or less significant anomalies in the land surface and middle tropospheric temperature, the mass field and the upper air wind field. The interannual variability at midlatitudes is governed by chaotic dynamics which are modulated by teleconnections in association with ENSO. In the following the model's skill in representing this aspect will be discussed in order to clarify what we can expect from the coupled model.

According to observations in Europe analysed by Fraedrich and Müller (1992), El Niño conditions lead to a cooling at the 850 hPa level in central and northern Europe in winter, which goes to zero in the region of the Black Sea and the Caspian Sea. There is a corresponding warming in La Niña situations. Roeckner et al. (1996a) compared the strength of teleconnection patterns associated with El Niño events in an ECHAM4-AMIP integration (with prescribed observed SSTs) in the boreal winter with those in the coupled model integration ECHAM4-OPYC3 used here, and with those in the ECMWF reanalysis. Both model integrations show considerable skill in representing the teleconnection patterns over the Pacific, where lower mean surface pressure corresponds to the warm phase of the ENSO and higher pressure to the cold phase. The difference patterns for El Niño cases also represent the teleconnections in the 500 hPa geopotential and temperature fields over North America and the North Atlantic (May and Bengtsson, 1996).

In Europe and Asia there is less agreement between the model simulations and the ECMWF reanalysis. The differences may be due to both deficiencies in the ECMWF reanalysis data set due to the limited sample and/or model errors in the simulations. In the reanalysis a cooling is

simulated in Europe as observed, but it is shifted to the south. Both the ECHAM4-AMIP and the ECHAM4-OPYC3 simulations show a weak response also in central to northern Europe. The response given by the reanalysis is negative to the west of the Ural mountains and positive between there and the Pacific in a large-scale pattern. In the ECHAM4-AMIP simulation this positive anomaly is placed farther south than in the reanalysis but is of the observed magnitude, while the ECHAM4-OPYC3 simulation represents a fraction of the observed magnitude, but places it more correctly to the north (Roeckner et al., 1996a).

As mentioned above, the ECHAM4-OPYC3 model overemphasizes the biennial component of the tropical circulation. In the ENSO-ensemble strong monsoons are those that are followed by a La Niña event. Therefore there is a greater likelihood of the occurrence of El Niño conditions in the preceding winter in the ensemble than in reality, and this is reflected in the sea surface temperature fields (not shown). In Europe we would then expect a cooling in mid-latitudes in winter (DJF) as a response to these El Niño conditions (Fraedrich and Müller, 1992). The winter surface temperature (not shown) in the ENSO-monsoon ensemble (DJF), however, shows positive Pacific SST anomalies occurring in conjunction with a non-significant warming in Europe. This means that the ENSO signal in the coupled model is not transferred in the way we would expect and chaotic mid-latitude dynamics seem to predominate. A significant anomaly pattern in surface temperature is established later in the spring (MAM) when east Pacific SST anomalies are less widespread. In the non-ENSO ensemble, the land surface temperature in Eurasia in MAM preceding the strong monsoon undergoes a general warming at the same position as in the other ensemble but without the presence of an El Niño signal in the Pacific.

4.2.4. The Eurasian Snow Cover

The reduced level of variability over the land has consequences for the investigation of the connection between the monsoon and the snow pack over Eurasia. Blanford (1884) hypothesized that anomalous snow over the Tibetan Plateau influences the strength of the subsequent monsoon. When satellite data of the snow pack became available (Hahn and Shukla, 1976; Dickson, 1984; Khandekar, 1991; Sankar-Rao et al., 1996) this hypothesis was extended to the continental scale of Eurasia. In years with anomalously large snow cover, the atmosphere is colder over land during the winter season, which causes a weak monsoon in the subsequent summer (Sankar-Rao et al., 1996). The inverse relationship between Eurasian snow cover anomalies and the Indian monsoon was confirmed by studies using long time series of snow cover from satellite (visible imagery from NOAA) (Yang, 1996). The same analysis also shows that the inverse relationship is not valid in ENSO winters, in which, for exzmple, the snow pack over Eurasia may increase due to the teleconnections from contemporaneous Pacific SSTs (Corti et al., 1998).

Results of model sensitivity studies are reviewed by Barnett et al. (1989), Yasunari et al. (1991), Vernekar et al. (1995), and Douville and Royer (1996). Temperature differences of only about 1.5 K over a small region at the surface in Tibet may cause an anomalous monsoon in model simulations (Vernekar et al., 1995). Dümenil and Bauer (1998) find that the systematic errors in that region in a hierarchy of MPI GCMs at various resolutions with different parameterisation schemes are of the same order, and that they have an influence on the strength of the monsoon in the model simulations. The difference between ECMWF and NCEP reanalyses over the Himalayas is also of the same order.

In association with the significant warming in Western Siberia in the coupled model integration one might expect to find a snow depth anomaly as well (Sankar-Rao, 1996), but the model simulated snow anomaly is not significant. The patterns of the anomalies in the snow depth field (in terms of water equivalent) in the model simulation are similar for the ENSO- and non-ENSO ensembles. The anomalies are not homogeneous at the continental scale but show some large-scale structure: Strong monsoons are distinguished from weak monsoons by smaller snow amounts in Western Eurasia and higher amounts in central Eurasia, reminiscent of the patterns given by Corti et al. (1998) for ensembles of ECMWF winter seasonal forecasts. These anomalies persist until the spring.

The fidelity of the model snow anomalies is difficult to validate. They have to be validated against the background of the model snow climatology and interannual variability. A large number of different model types (and among them the atmospheric ECHAM model) was found to strongly underrepresent the interannual variability of Eurasian snow when they were forced with observed SSTs (Frei et al., 1998). Satellite based estimates of snow cover have been assessed to be reliable, but snow depth from satellite still shows many systematic erros (Foster et al., 1996; Bamzai and Kinter, 1998) and the available time series is still relatively short.

Although the reanalyses provide a useful synopsis of global atmospheric fields, they cannot be used for the validation of land surface processes. In general the reanalyses do not give a faithful representation of the climatology or of the interannual variability of the hydrological cycle at the land-surface (Stendel and Arpe, 1997), and show particular deficiencies with regard to snow. These deficiencies result from the fact that prior to 1991 hardly any observations of snow cover and snow depth were available to the ECMWF reanalyses in large parts of Eurasia (Viterbo, 1997, personal communication). The ECMWF assimilation system therefore uses a climatology during those years. The ECMWF reanalysis shows an unrealistic pattern of snow depth variation between strong and weak monsoon years with no differences to the east of the Ural mountains. In the NCEP reanalysis, the snow cover of the relatively anomalous year of 1973 was used in every year from 1974 to 1994; hence only 1973, 1995 and 1996 have a snow cover that is consistent with the atmospheric observations. These aspects may not be damaging to the quality of the atmospheric circulation fields which are the most important products of the

reanalysis, because some information is still retained in the low level assimilated variables, but they are particularly detrimental to the study of the variability caused by processes at the land surface in Eurasia.

In order to overcome the problem of the incomplete database for snow depth, Corti et al. (1988) have created a surrogate snow depth climatology from ensembles of winter seasonal forecasts with the ECMWF model. The authors find a significant association between the positive/negative phase of the snow depth and circulation anomalies and warm/cold ENSO events. The present coupled model simulation indicates increased snow amounts over continental scale Eurasia in El Niño years and less in La Niña years, but the strong or weak monsoons are not distinguished by significant anomalies of snow depth.

Due to an overestimation of the surface elevation at one gridpoint, the snow mass in Tibet is erroneously large in the model simulation. This has an influence on the general climatology of the monsoon because it leads to too cold temperatures persisting into the spring months (Dümenil and Bauer, 1998). The effect of continental scale snow mass, however, seems to be relatively unimportant for the interannual variability of the monsoon in the coupled model, because it is counteracted by the erroneous development of Indian Ocean SST anomalies in the monsoon year. As is so often the case, here two systematic errors seem to work in opposite directions so that the monsoon variability is not too unrealistic in the present model simulation, but this aspect requires further model development. The interannual variation of the snow depth in the model is not sufficently well represented to study further ensembles of high vs. low snow amount cases and how they are related to the Indian monsoon.

4.3 The Post-Monsoon Season

At the end of the monsoon season (SON), the Indian Ocean SST (not shown) is cooler than normal in strong monsoon cases, in the ENSO ensemble as well as the non-ENSO ensemble. These significant anomalies in the immediate vicinity of the Indian subcontinent can be attributed to the influence of the monsoon rather than to that of the ENSO. Considering only the action of the monsoon, stronger monsoons would create a stronger atmospheric flow from the ocean to the continent and more upwelling, and this would lead to a cooling of the ocean. But again, this feature is simulated against the background of a systematic model error concerning the very small interannual variation of Indian Ocean SST, and therefore no final conclusion is possible on the question of feedbacks with Indian Ocean SSTs.

In India the model-simulated non-ENSO monsoons show a small-scale warming at the surface over land in DJF preceding the monsoon. It is due to the persistence of a soil moisture and heat anomaly caused by the anomalously weak monsoon of the previous summer. This anomaly dominates the local processes under both the ENSO as well as non-ENSO conditions. It is also a much larger anomaly than the one found in the ECMWF reanalysis. Due to the various

problems concerning the land surface hydrology (Stendel and Arpe, 1997), the analysed soil moisture field cannot, however, be judged to be reliable. In both the ENSO and non-ENSO cases the local cold anomaly in JJA over India is accompanied by a significant warm anomaly in the Himalayas. The fact that the monsoon is strong in the case of the wet and cold anomaly locally over India indicates that it is not the surface temperature that determines the overall strength of the monsoon, but rather the temperature at levels just above the highlands of Tibet (Flohn, 1964). Secondly, the regional land surface anomaly is potentially more important at the time of the onset of the monsoon than for the remainder of the monsoon season.

The significant near-surface cooling due to a strong monsoon and warming due to a weak monsoon over land in India persists until the following winter. The regional heat anomaly is certainly model dependent and may lead to feedbacks that may modulate the variation of the monsoon (Meehl, 1994). A realistic lifetime of such anomalies cannot be validated due to the lack of data. In the model, the land surface is saturated and cools relatively early in the monsoon season, i.e. already in JJA. In the reanalysis, saturation occurs only towards the end of the monsoon season (SON), suggesting that there are large differences between the treatment of the hydrological cycle at the land surface.

5. Summary and Conclusions

The performance the ECHAM4-T42-OPYC3 model was diagnosed with regard to the representation of the interannual variability of the Indian summer monsoon. The aim of the study was to investigate if there are anomalous monsoons in the model simulation that do not coincide with ENSO events and, if there are, how they differ from anomalous monsoons that occur in the summer when an ENSO event is developing in the Pacific. This is discussed on the basis of two composites of strong and weak monsoons, first with respect to the influence of SST anomalies during the various states of the El Niño-Southern Oscillation, and second, the influence from the land surfaces in the absence of Pacific SST anomalies. In this study a set of diagnostics was developed which gives a qualitative as well as quantitative measure of the skill of the model simulation. For the validation of atmospheric fields the ECMWF reanalysis was used.

Several criteria were applied to determine whether a monsoon is strong or weak. Taking advantage of the fact that the correlation of rainfall in the Indian region with the large-scale monsoon index of Webster and Yang (1992) is as high at the land points as at the adjacent ocean gridpoints, a new regional average of rainfall was developed from the reanalysis data in this study. Although the mean precipitation in the coupled model over India is slightly deficient, the level of interannual variability according to this regional criterion is similar to observations.

The model gives a coherent picture of processes and interactions which are within the range of uncertainty of the observations. In particular, the occurrence of ENSO events and associated monsoon anomalies is very well simulated. Strong monsoons often occur during years of a developing La Niña event, while weak monsoons often occur in the summers prior to a mature El Niño. This relationship was not well represented in earlier coupled models (Latif et al., 1994). The half-yearly reversal of the circulation is essentially driven by the differential heating between the Asian land mass and the Indian Ocean during the annual cycle which causes the ITCZ to be diverted towards the Indian subcontinent. In some years the temperature gradient is varied by the action of the land surface, in other years by the action of the Indian or Pacific Ocean, and in yet other years by the net effect of the two.

The interactions between the land, ocean and the monsoon circulation are manifold. Developing ENSO events may have a direct effect via an east- or westward shift of the centers of convection associated with the Walker circulation during the summer months. In winter, during the mature stage of the ENSO, the teleconnections are found to reach into the North Atlantic/-European/Eurasian sector which may lead to an increase or decrease in land surface temperatures and/or the snow pack. This indirect effect of the ENSO phenomenon, together with the chaotic dynamics at middle and high latitudes, may imprint the previous winter's conditions in the 'memory' of the land surface and therefore lead to variations in the strength of the subsequent monsoon.

In order to separate the potential influence from the land surface from that of the Pacific SST anomalies, two ensembles of strong and weak monsoons were studied: One where SST anomalies in the Pacific are nil and one where SST anomalies of the ENSO type occur in the Pacific. In both ensembles strong monsoons are distinguished from weak monsoons by equally large local precipitation anomalies in the Indian sector. These appear in conjunction with consistent large-scale anomalies in the tropical easterly jet and the 200 hPa velocity potential. Changes in the strength of the subtropical jet are found in both hemispheres. In the non-ENSO ensemble where there is no Pacific Ocean SST anomaly, these wind anomalies appear in the summer in the entrance region of the tropical easterly jet and are associated with small local tropospheric temperature anomalies in the Indian Ocean and West Pacific. In both ensembles at mid-tropospheric levels a continental temperature anomaly south of 30°N, caused either by the chaotic dynamics of the midlatitudes or modulations through ENSO events, is accompanied by an anomaly of opposite sign over the Indian Ocean. The origin of this relatively small Indian Ocean anomaly in the non-ENSO related monsoons requires further investigation, and in the ENSO-ensemble it appears to be associated with the evolution of ENSO events during the annual cycle in the Pacific. We know from the comparison with observed SST datasets that the model simulated Indian Ocean SST anomaly is of too small amplitude in the ENSO-related cases. As the model simulated Pacific SSTs display a too strong biennial variation, the transition from negative to positive atmospheric and land anomalies during the annual cycle is different

from the average development in the observations. In particular this reduces the Indian Ocean SST anomalies in the spring which is critical for the development of monsoon anomalies. This is one of the two serious systematic model errors with regard to the interannual variability of the monsoon in the spring, the most decisive point in time for the development of monsoon anomalies.

The second error concerns the spring snow cover in Eurasia. Teleconnections from the ENSO events are found in North America and the North Atlantic/European area. In ENSO winters, the model produces more snow in Eurasia, but there is no significant snow pack anomaly in years preceding anomalous monsoons. Our model results in this respect disagree with the results from the coupled model of Meehl (1994) who showed an impact from a much smaller snow pack anomaly than ours. This cannot be investigated further at this point, because the reanalysis does not exhibit any variability in the region of interest, and station observations from Russia which recently have become available do not show any correlation with precipitation in India (Arpe, 1997, personal communication).

In the monsoon season near-surface wind anomalies are found in the West Pacific in ENSO-related monsoon cases and in non-ENSO cases as well. This means that the action of the monsoon wind field anomalies may interact with ocean dynamics in the Western Pacific even if the monsoon is not itself influenced by contemporaneous Pacific SST anomalies.

Further studies will address the role of tropical convection on monsoon interannual variability. A number of deficiencies concerning the data base for such studies and systematic errors of the coupled model simulation have been identified in this study. Model development in the future should focus on improvement of the monsoon climatology, mainly via the parameterisation schemes. As some of the systematic errors involving the monsoon-ocean interaction may be masking each other, it has to be expected that many of the results discussed above are model dependent. The interaction between the ENSO and the strength of the monsoon will be part of a model intercomparison excercise in the Coupled Model Intercomparison Project (CMIP). It will be interesting to see how the validation of model results is changed when longer reanalyses and SST datasets are used. These would also provide an incentive to study decadal variations.

Acknowledgments. I would like to thank my colleagues at the Max-Planck-Institut für Meteorologie for their support and discussions. Special thanks are due to Erich Roeckner who generously provided the model data, to Uwe Schulzweida who processed the data and designed the figures and to Klaus Arpe who provided snow correlation maps.

References

Arpe, K., L. Dümenil and M. Giorgetta, 1998, Variability of the Indian monsoon in the ECHAM3 model, sensitivity to sea surface temperature, soil moisture and the stratospheric QBO. J. Climate (in press).

Bamzai, A.S. and J.L. Kinter III, 1997, Climatology and interannual variability of Northern Hemisphere snow cover and depth based on satellite observations. COLA Report No. 52, Center for Ocean-Land-Atmosphere Studies, Calverton, MD, 26pp.

Bamzai, A. and J. Shukla, 1998, Relation between Eurasian snow cover, snow depth and the Indian summer monsoon: an observational study. COLA Report No. 53, Center for Ocean-Land-Atmosphere Studies, Calverton, MD, 33pp.

Barnett, T.P., L. Dümenil, U. Schlese, E. Roeckner and M. Latif, 1989, The effect of Eurasian snow cover on regional and global climate variations. J. Atmos. Sci., 46, pp. 661-685.

Bengtsson, L., K. Arpe, E. Roeckner and U. Schulzweida, 1996, Climate predictability experiments with a general circulation model. Climate Dyn., 12, pp. 261-278.

Blanford, H.F., 1884, On the connexion of the Himalayan snowfall with dry winds and seasons of droughts in India. Proc. Roy. Soc. London, 37, pp. 3-22.

Charney, J.G. and J. Shukla, 1981, Predictability of monsoons. In: Monsoon Dynamics. Eds. J. Lighthill and R. Pearce, Cambridge University Press, Cambridge, pp. 99-109.

Corti, S., F. Molteni and C. Brancovic, 1998, Predictability of snow-depth anomalies over Eurasia and associated circulation patterns. Submitted to Quart. J. Roy. Meteor. Soc.

Das, P.K., 1986, Monsoons. WMO. No. 613, World Meteorological Organization, Geneva, 155pp.

Dickson, R.R., 1984, Eurasian snow cover versus Indian monsoon rainfall - an extension of the Hahn-Shukla results. J. Climate Appl. Meteor., 23, 171-173.

Douville, H. and J.-F. Royer, 1996, Sensitivity of the Asian summer monsoon to an anomalous Eurasian snow cover within the Meteo-France GCM. Climate Dyn., 121, pp. 449-466.

Dümenil, L. and E. Roeckner, 1992, Sensitivity of GCM simulations of the northern hemisphere monsoon circulations of 1987 and 1988 to sea surface temperature changes. Report of workshop on Simulation of Interannual and Intraseasonal Monsoon Variability. WCRP-68, WMO/TD-No. 470, World Meteorological Organization, Geneva, pp. 2.31-2.36.

Dümenil, L. and H.-S. Bauer, 1998, The tropical easterly jet in a hierarchy of GCMs and in reanalyses. Max-Planck-Institute Report No. 247, Hamburg, 45pp. Submitted to J. Meteor. Soc. Japan.

Flohn, H., 1964, Investigations on the tropical easterly jet. Bonner Meteor. Abhandl., 4, pp. 1-69.

Foster, J., G. Liston, R. Koster, R. Essery, H. Behr, L. Dümenil, D. Verseghy, S. Thompson, D. Pollard and J. Cohen, 1996: Snow cover and snow mass intercomparisons of general circulation models and remotely sensed datasets. J. Climate, 9, pp. 409-426.

Fraedrich, K. and K. Müller, 1992, Climate anomalies in Europe associated with ENSO extremes. Int. J. Climatol., 12, pp. 25-31.

Frei, A., A. Robinson and AMIP Modeling Group, 1998: Evaluation of snow extent and its variability in the Atmospheric Model Intercomparison Project. Submitted to J. Geophys. Res.

Gates, W.L., 1992, AMIP: The Atmospheric Model Intercomparison Project. Bull. Am. Meteor. Soc., 73, 12, pp. 1962-1970.

Gibson, J.K., P. Kallberg, S. Uppala, A. Hernandez, A. Nomura and E. Serrano, 1997, The ECMWF Re-Analysis (ERA). 1. ERA description. ECMWF Re-Analysis Project Report Series No. 1, European Centre for Medium-Range Weather Forecasts, Reading, U.K., 71pp.

Hagemann, S. and L. Dümenil, 1998: Development of a parameterization of lateral discharge for the global scale. Climate Dyn., 14, 1, pp. 17-31.

Hahn, D.J. and J. Shukla, 1976, An apparent relationship between Eurasian snow cover and Indian monsoon rainfall. J. Atmos. Sci., 33, pp. 2461-2462.

Joseph, P.V., J.K. Eischeid and R.J. Pyle, 1994, Interannual variability of the onset of the Indian summer monsoon and its asssociation with atmospheric features, El Niño, and sea surface temperature anomalies. J. Climate, 7, pp. 81-105.

Ju, J. and J. Slingo, 1995, The Asian summer monsoon and ENSO. Quart. J. Roy. Meteor. Soc., 121, pp. 1133-1168.

Kalnay, E., M. Kanamitsu, R. Kistler, W. Collins, D. Deaven, L. Gandin, M. Iredell, S. Saha, G. White, J. Woollen, Y. Zhu, M. Chelliah, W. Ebisuzaki, W. Higgins, J. Janowiak, K.C. Mo, C. Ropelewski, J. Wang, A. Leetmaa, R. Reynolds, R. Jenne and D. Joseph, 1996, The NCEP/NCAR 40-year reanalyses project. Bull. Am. Meteor. Soc., 77, pp. 437-471.

Khandekar, M.L., 1991, Eurasian snow cover, Indian monsoon and ElNiño/Southern Oscillation - a synthesis. Atmos.-Ocean, 29, pp. 636-647.

Kripalani, R.H., 1996, Assessing the impact of El Niño and non-El Niño-related droughts over India. Drought Network News, pp. 11-13.

Latif, M., A., A. Sterl, M. Assenbaum, M.M. Junge and E. Maier-Reimer, 1994, Climate variability in a coupled GCM. Part II: The Indian Ocean and monsoon. J. Climate., 7, pp. 1449-1462.

May, W. and L. Bengtsson, 1996, On the impact of the El Niño/Southern Oscillation phenomenon on the atmospheric circulation in the northern hemisphere extratropics. Max-Planck-Institute Report No. 224, Hamburg, 61pp.

Meehl, G.A., 1987, The annual cycle and interannual variability in the tropical Pacific and Indian Ocean regions. Mon. Wea. Rev., 115, pp. 27-50.

Meehl, G.A., 1994, Coupled land-ocean-atmosphere processes and south Asian monsoon variability. Science, 265, pp. 263-267.

Meehl, G.A., 1994, Influence of the land surface in the Asian summer monsoon: External conditions versus internal feedbacks. J. Climate, 7, pp. 1033-1949.

Mooley, D.A. and J. Shukla, 1987, Variability and forecasting of the summer monsoon rainfall over India. In: Monsoon meteorology. Eds. Chang, C.-P. and T.N. Krishnamurti, Oxford University Press, Oxford, pp. 26-59.

Normand, C., 1953, Monsoon seasonal forecasting. Quart. J. Roy. Meteor. Soc., 79, 342, pp. 463-473.

Oberhuber, J.M., 1993, Simulation of the Atlantic circulation with a coupled sea ice - mixed layer - isopycnal general circulation model. Part I: Model description. J. Phys. Oceanogr., 22, pp. 808-829.

Palmer, T.N., C. Brancovic, P. Viterbo and M.J. Miller, 1992, Modelling interannual variations of summer monsoons. J. Climate, 5, pp. 399-417.

Parthasarathy, B., A.A. Munot and D.R. Kothawale, 1994, All-India monthly and seasonal rainfall series: 1871-1993. Theor. Appl. Climatol., 49, pp. 217-224.

Prell, W.L., and J.E. Kutzbach, 1992: Sensitivity of the Indian monsoon to forcing parameters and implications for its evolution, Nature, 360, pp. 647-651.

Quinn, W.H., V.T. Neal and S.E. Antunez de Mayolo, 1987, El Niño occurrences over the past four and a half centuries. J. Geophys. Res., 92, pp. 14 449-14 461.

Rasmusson, E.M. and T.H. Carpenter, 1983, The relationship between eastern equatorial Pacific sea surface temperatures and rainfall over India and Sri Lanka. Mon. Wea. Rev., 111, pp. 517-528.

Rayner, N.A., E.B. Horton, D.E. Parker, C.K. Folland, and R.B. Hackett, 1996, Version 2.2 of the global sea-ice and sea surface temperature dataset, 1903-1994. Climate Research Technical Note CRTN 74, Hadley Centre, Bracknell.

Reynolds, R.W. and T.M. Smith, 1994, Improved global sea surface temperature analysis using optimum interpolation. J. Climate, 7, pp. 929-948.

Roeckner, E., J.M. Oberhuber, A. Bacher, M. Christoph and I. Kirchner, 1996a, ENSO variability and atmospheric response in a global coupled atmosphere-ocean GCM. Climate Dyn., 12, pp. 737-754.

Roeckner, E., K. Arpe, L. Bengtsson, M. Christoph, M. Claussen, L. Dümenil, M. Esch, M. Giorgetta, U. Schlese and U. Schulzweida, 1996b: The atmospheric general circulation model ECHAM4: Model description and simulation of present-day climate. Max-Planck-Institut für Meteorologie Report No. 218, Hamburg, 90pp.

Rudolf, B., H. Hauschild, M. Reiß and U. Schneider, 1992, The calculation of areal mean precipitation totals on a 2.5 grid by an objective analysis method. Meteor. Z., N.F. 1, pp. 32-50.

Sankar-Rao, M., K.M. Lau and S. Yang, 1996, On the relationship between Eurasian snow cover and the Asian monsoon. Int. J. Climatol., 16,pp. 605-616.

Shukla, J. and D.A. Paolino, 1983, The Southern Oscillation and long-range forecasting of the summer monsoon rainfall over India. Mon. Wea. Rev., 111, pp. 1830-1837.

Sontakke, N.A., G.B. Pant and N. Singh, 1993, Construction of all-India summer monsoon rainfall series for the period 1844-1991, J. Climate, 6, pp. 1807-1811.

Sperber, K.R. and T.N. Palmer, 1996, Interannual tropical rainfall variability in general circulation model simulations associated with the Atmospheric Model Intercomparison Project. J. Climate, 9, pp. 2727-2750.

Stendel, M. and K. Arpe, 1997, Evaluation of the hydrological cycle in reanalyses and observations. Max-Planck-Institut für Meteorologie Report No. 228, 52 pp.

Torrence, C. and P.J. Webster, 1995, Low frequency variability and the annual cycle. In: Proceedings of the International TOGA Conference, Melbourne, Australia (1-7 April 1995), WCRP-91, WMO-TD. No. 717, World Meteorological Organization, Geneva, pp. 666-669.

Venzke, S., M. Latif and A. Villwock, 1997, The coupled GCM ECHO-2. Part II: Indian Ocean response to ENSO. Max-Planck-Institute für Meteorologie Report No. 246, 23pp.

Vernekar, A.D., J. Zhou and J. Shukla, 1995, The effect of Eurasian snow cover on the Indian Monsoon. J. Climate, 8, pp. 248-266.

Webster, P.J., 1995, The annual cycle and the predictability of the tropical coupled ocean-atmosphere system. Meteorol. Atmos. Phys., 56, pp. 33-55.

Webster, P.J. and S. Yang, 1992, Monsoon and ENSO: selectively interactive systems. Quart. J. Roy. Meteor. Soc., 118, pp. 877-926.

WMO, 1993, Simulation and prediction of monsoons - recent results. TOGA/WGNE Monsoon Numerical Experimentation Group, WCRP-80, WMO-TD. No. 546, World Meteorological Organization, Geneva.

Yang, S., 1996, ENSO-snow-monsoon associations and seasonal interannual predictions. Int. J. Climatol., 16, pp. 125-134.

Yang, S., K.M. Lau and M. Sankar-Rao, 1996, Precursory-signals associated with the interannual variability of the Asian summer monsoon. J. Climate, 9, pp. 949-964.

Yasunari, T., 1990, Impact of Indian monsoon on the coupled atmosphere/ocean system in the tropical Pacific. Meteorol. Atmos. Phys., 44, pp. 29-41.

Yasunari, T., 1991a, Monsoon and ENSO: a coupled ocean/land/atmosphere system. TOGA Notes, No. 2, pp. 9-13.

Yasunari, T., 1991b, The monsoon year - a new concept of the climatic year in the tropics. Bull. Amer. Meteor. Soc., 72, pp. 1331-1338.

Yasunari, T., A. Kitoh and T. Tokioka, 1991, Local and remote responses to excessive snow mass over Eurasia appearing in the northern spring and summer climate - a study with the MRI GCM. J. Meteor. Soc. Japan, 69, pp. 473-487.

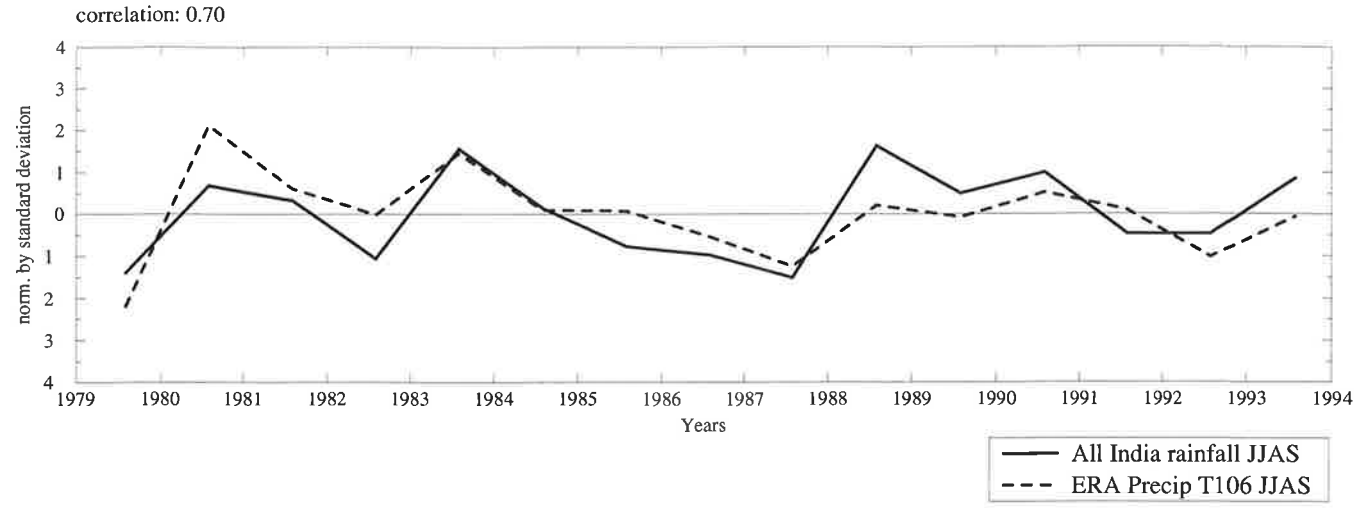

Fig. 1) Interannual variation of all-India rainfall for the monsoon season (June to September) and precipitation over land grid-points for India from the ECMWF-T106 reanalysis for 1979 to 1993. The correlation between the two time series is 0.70.

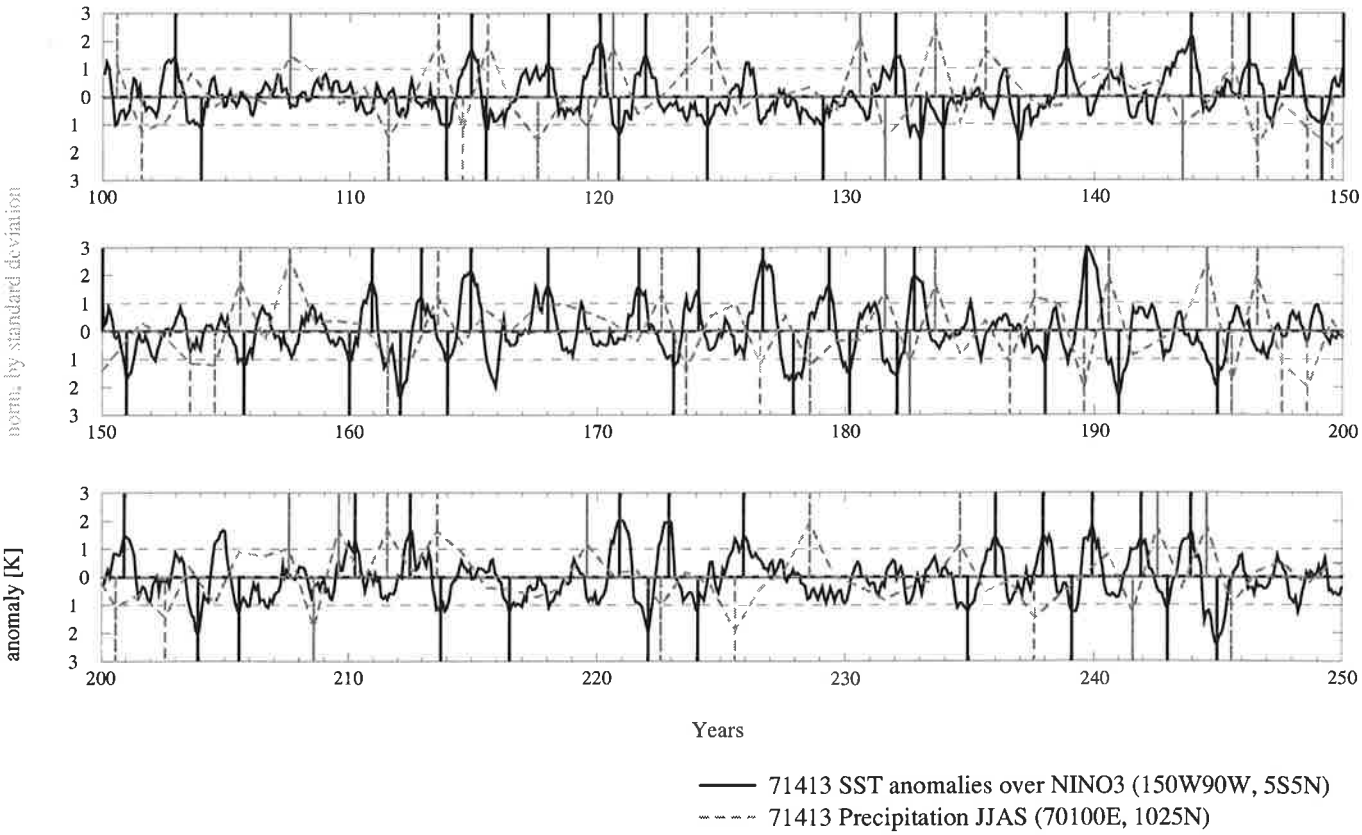

Fig. 2) Interannual variability of monthly mean NIÑO3 sea surface temperature (150W-90W, 5S-5N) and monsoon precipitation for June to September for the region (70E-100E, 10N-25N) computed from the 150 year-simulation of the ECHAM4-T42-OPYC3 model. Solid bars indicate occurrences of El Niño or La Niña events, thin bars indicate strong or weak monsoons according to the definitions given in the text.

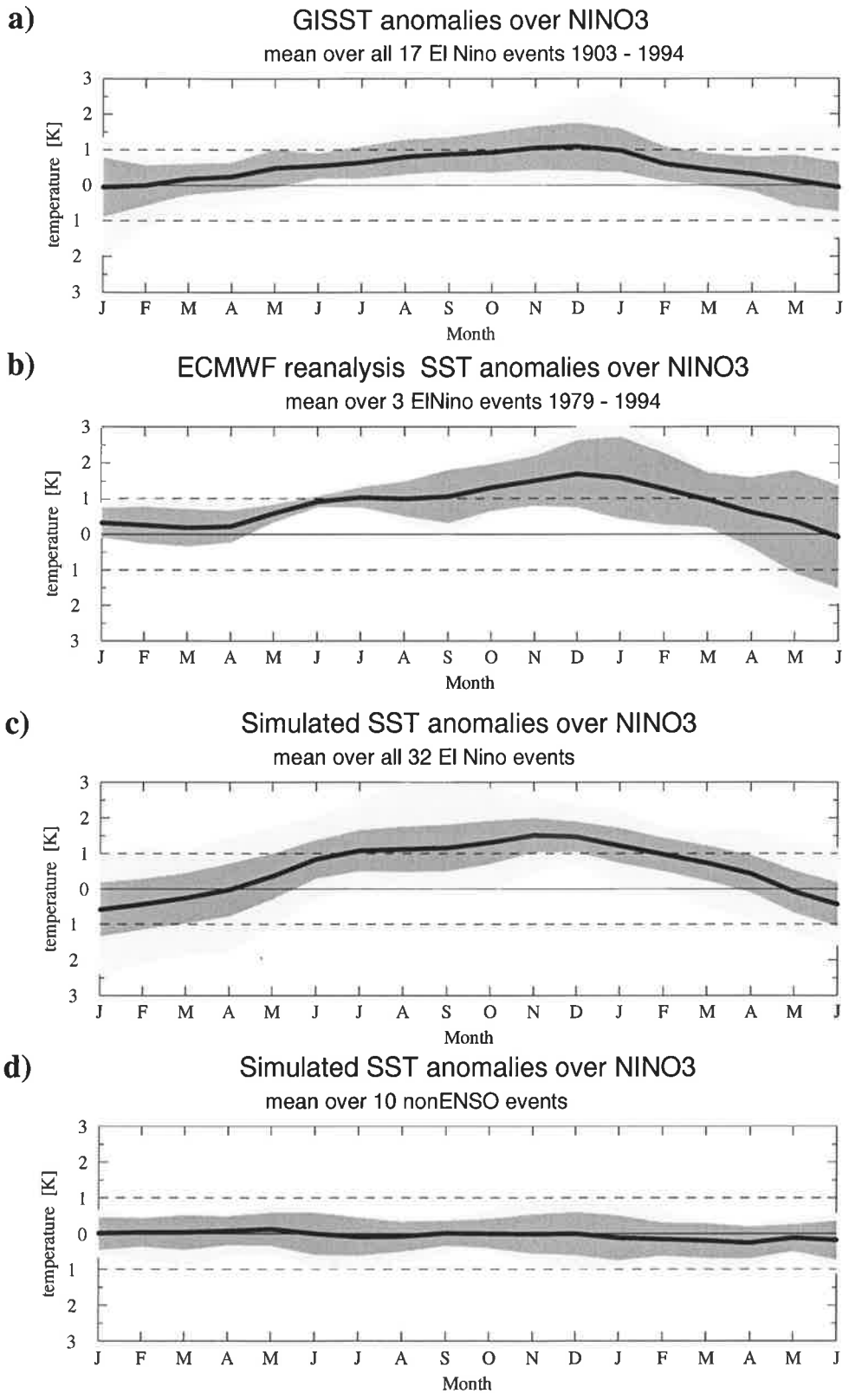

Fig. 3) Monthly mean NIÑO3 (5S-5N, 150W-90W) sea surface temperature anomalies averaged over:

a) 17 El Niño events from the GISST dataset (1903-1994) (Rayner et al., 1996)

b) 3 El Niño events from the ECMWF reanalysis 1979-1993

c) 32 El Niño events from the 150 year simulation with the ECHAM4-T42-OPYC3 model

d) 10 cases of near zero NIÑO3 anomalies in the 150 year simulation.

Shading indicates the range of variation within the ensemble, the standard deviation is shown in dark grey, the range of extreme values in light grey.

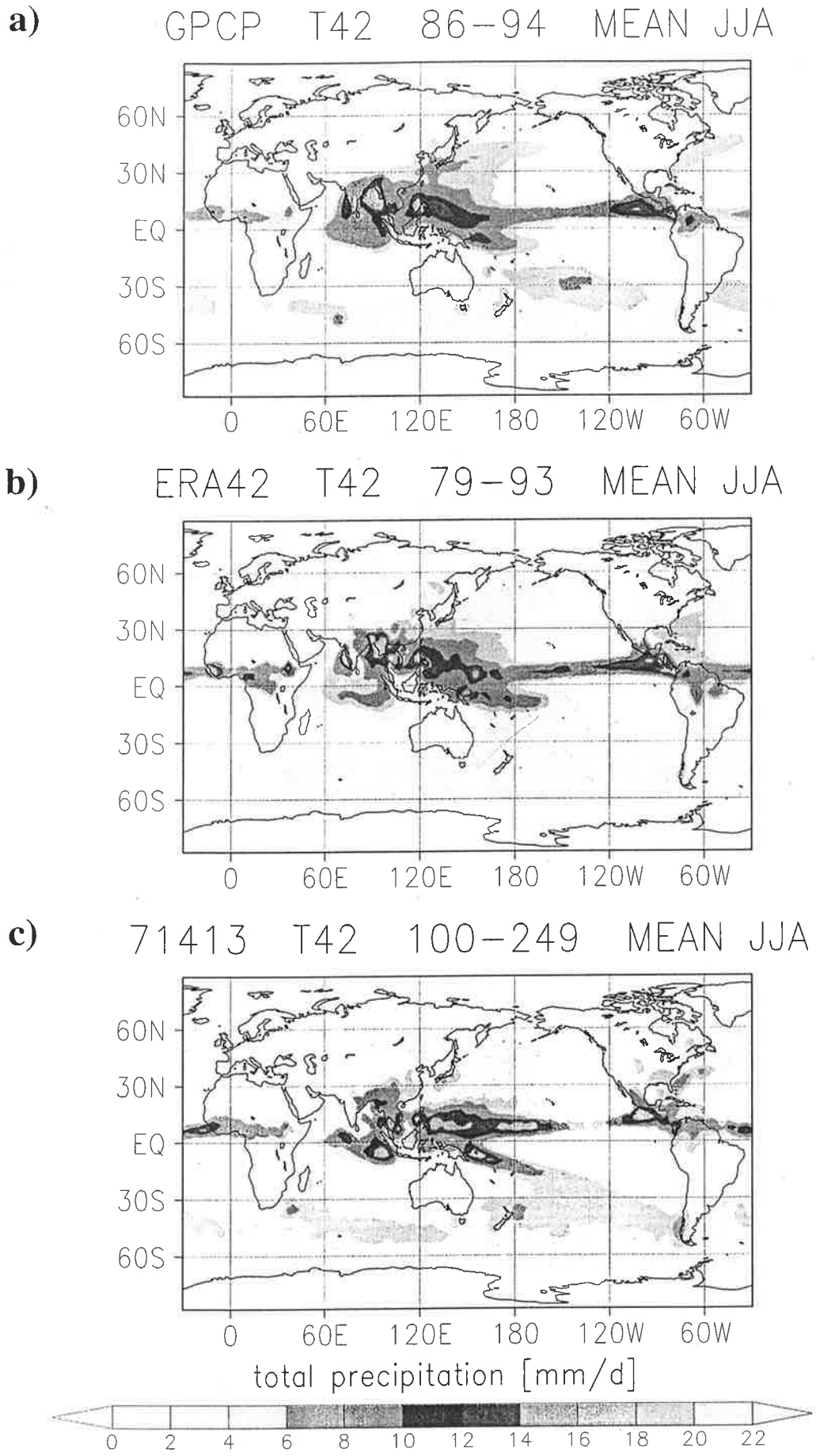

Fig. 4) Long-term average of the JJA precipitation field from

a) GPCP data (1986-94) (Rudolf et al., 1992)

b) the ECMWF reanalysis (1979-1993)

c) from the 150-year simulation with the ECHAM4-T42-OPYC3 model.

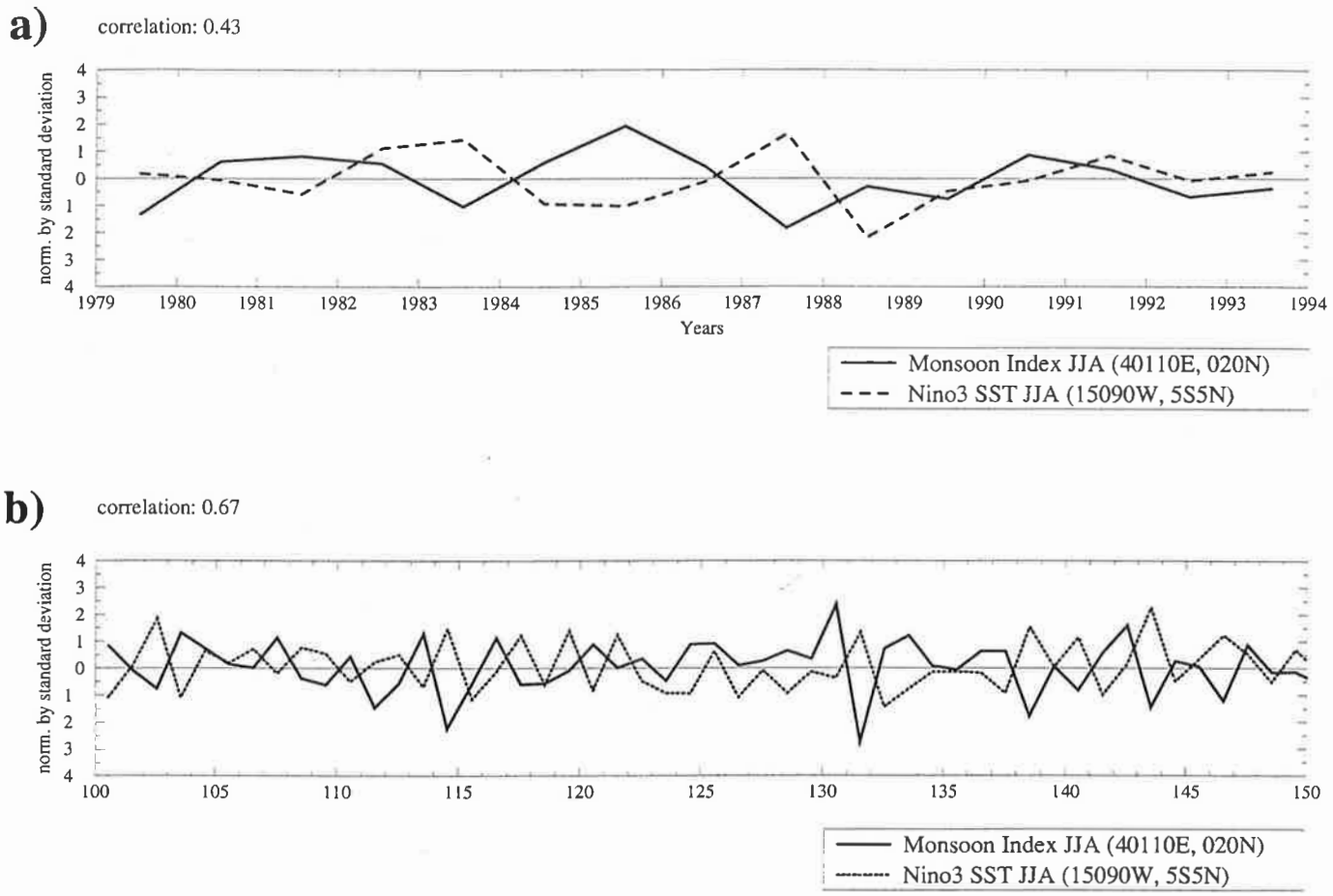

Fig. 5) Interannual variation of the monsoon index of Webster and Yang (1992) for the monsoon season June to August and NIÑO3 sea surface temperatures (5S-5N, 150W-90W) for June to August, computed:

a) from the ECMWF T106 reanalysis for the period 1979-1993 (the correlation between the two time series is -0.43),

b) from the 150-year simulation of the ECHAM4-T42-OPYC3 model (the correlation between the two time series is -0.67).

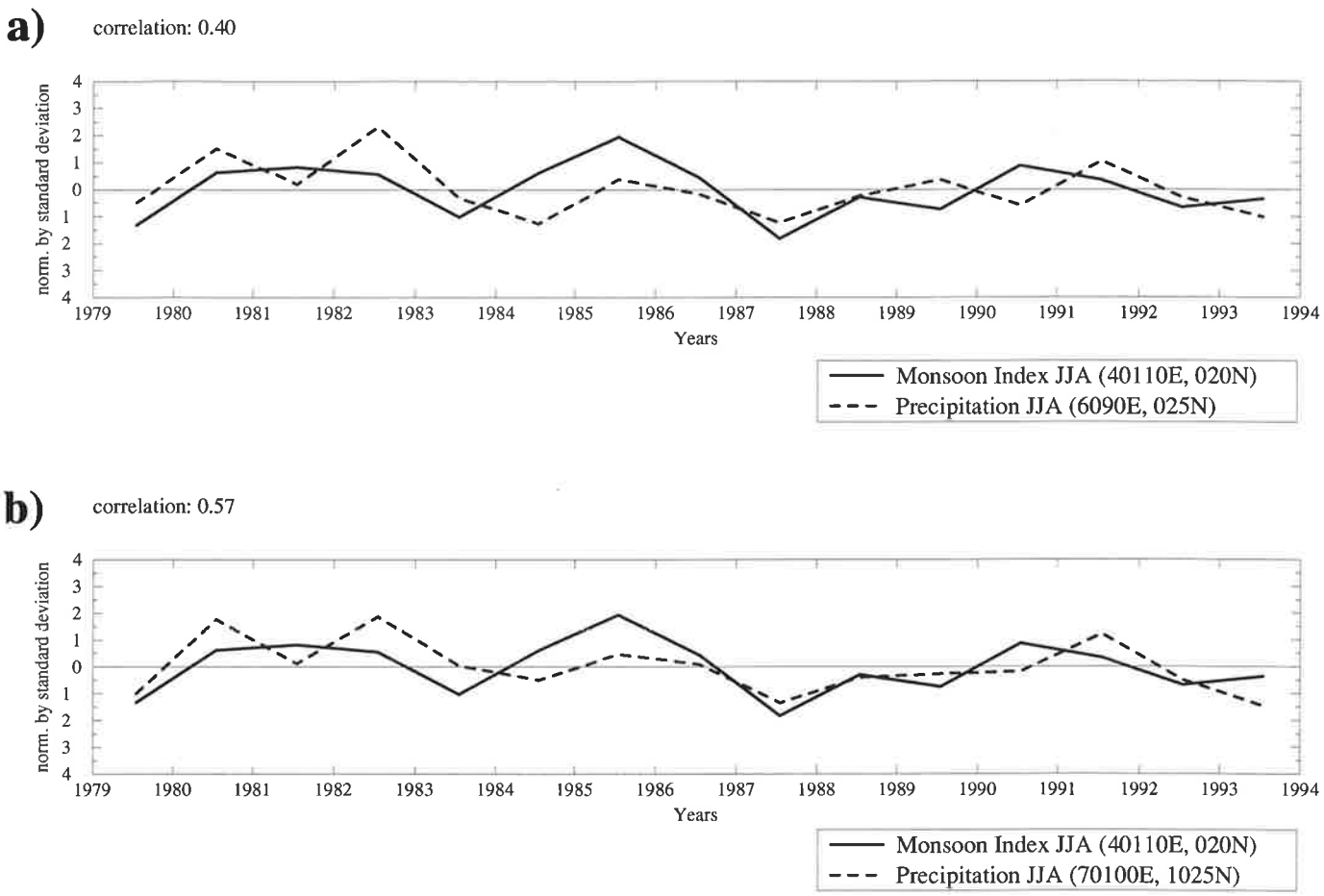

Fig. 6) Interannual variation of the monsoon index of Webster and Yang (1992) for the monsoon season June to August and

a) rainfall in the region (60-90E, 0-25N)

b) rainfall in the region (70-100E, 10-25N, land and ocean points included) computed from the ECMWF T106 reanalysis for the period 1979-1993.

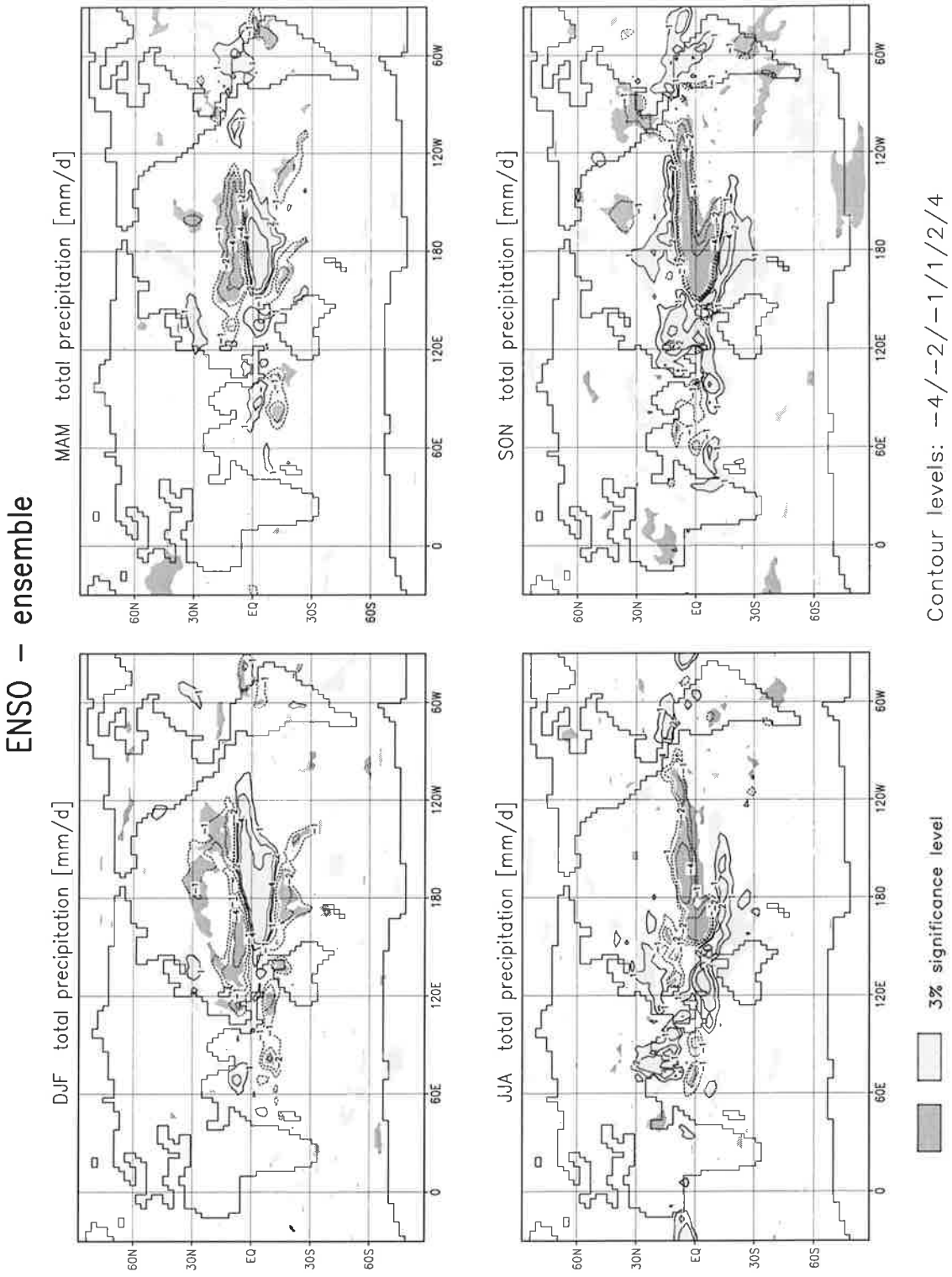

Fig. 7a) Difference of seasonal means of monsoon precipitation between strong and weak Indian monsoons in the ensemble of ENSO-monsoon years from the 150 year simulation with the ECHAM4-T42-OPYC3 model, when strong monsoons are followed by La Niña events and weak monsoons by El Niño events. Significance of results at 97% level in a Students´ t-test.

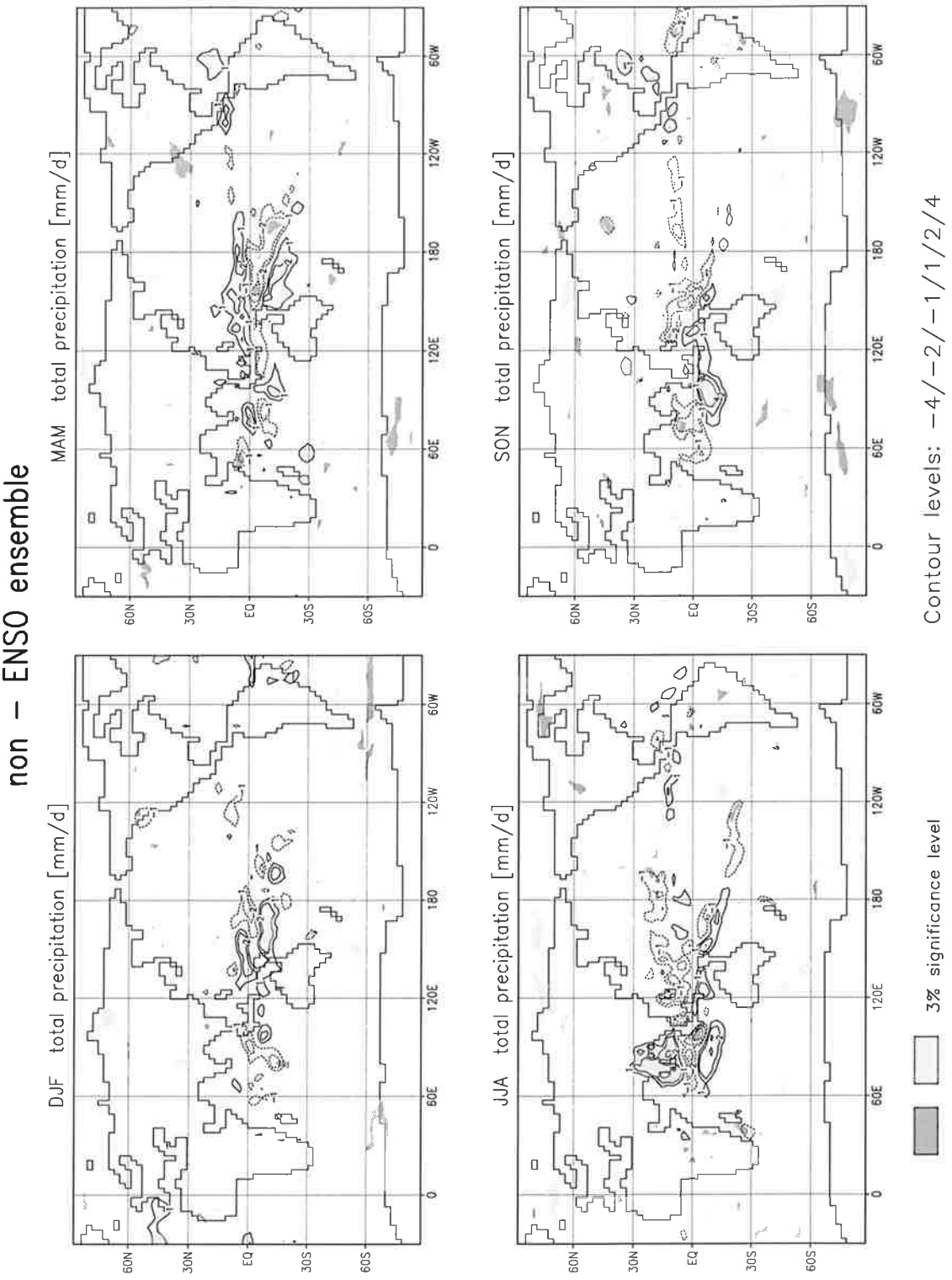

Fig. 7b) As 7a) but for the ensemble of 10 non-ENSO monsoon years from the 150 year simulation with the ECHAM4-T42-OPYC3 model.

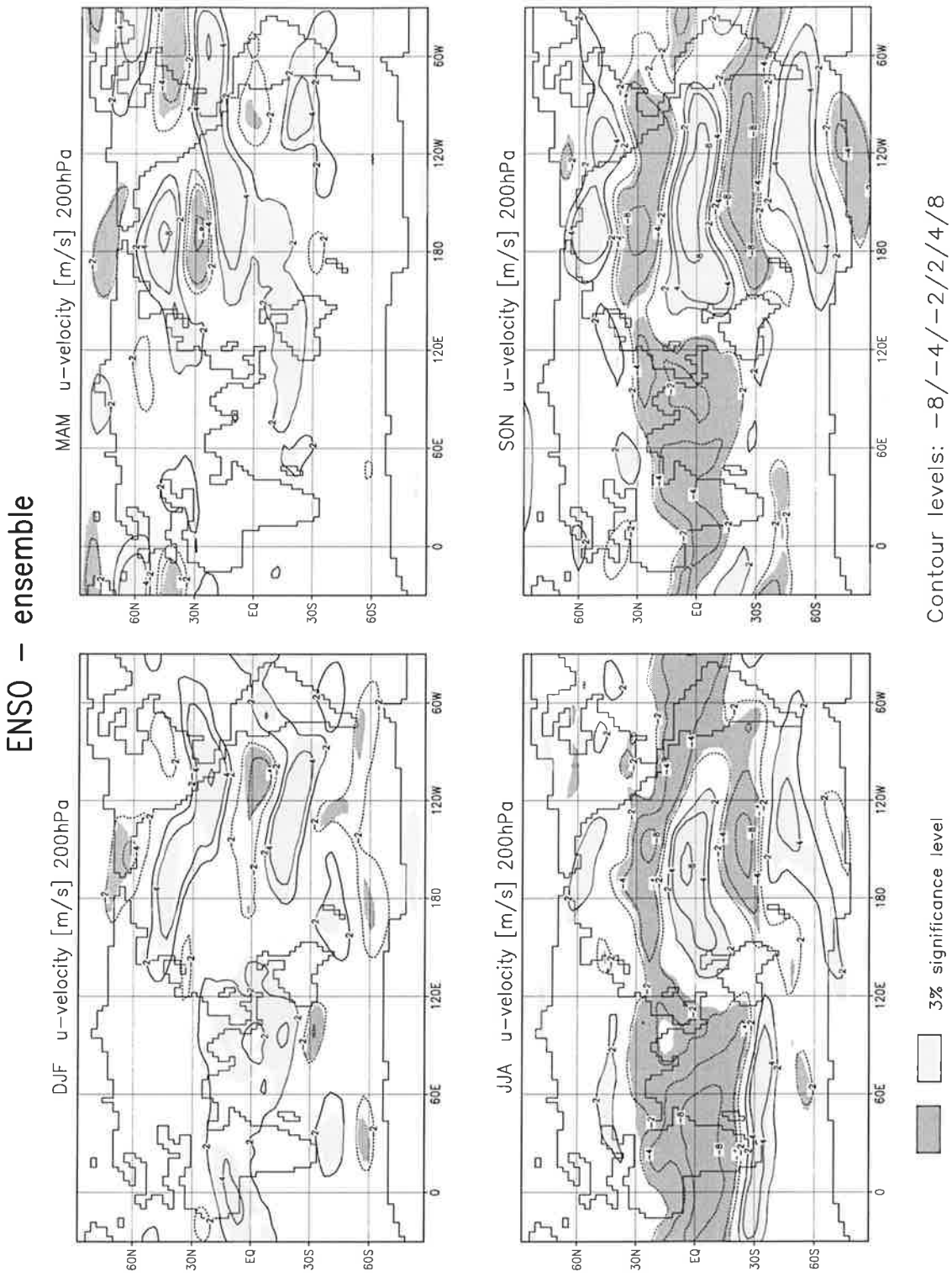

Fig. 8a) Difference of seasonal means of zonal wind velocity at 200 hPa between strong and weak Indian monsoon cases from the ensemble of ENSO-monsoon years. Significance of results at 97% level in a Students´ t-test.

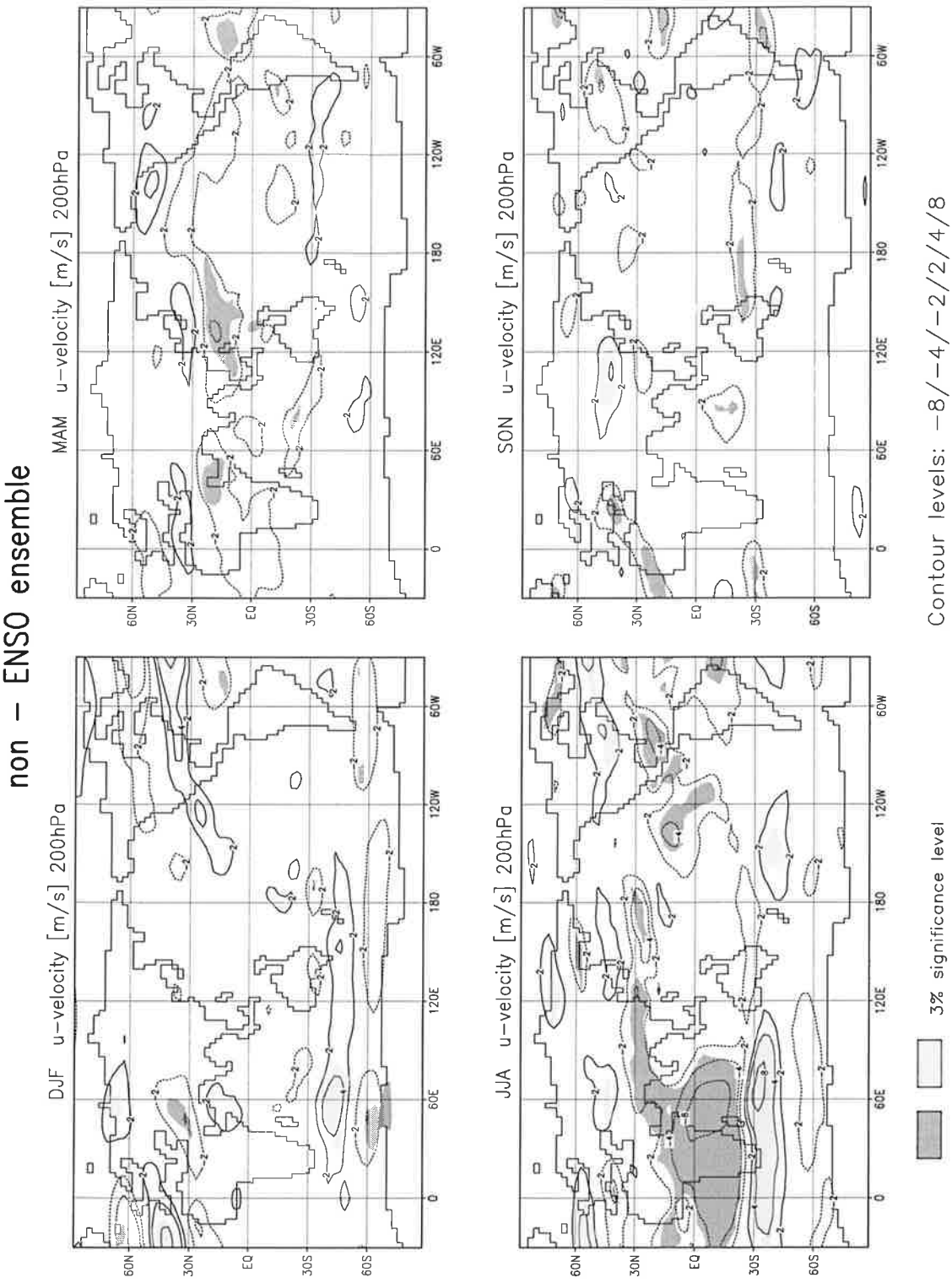

Fig. 8b) As 8a) but for the ensemble of non-ENSO-monsoon years.

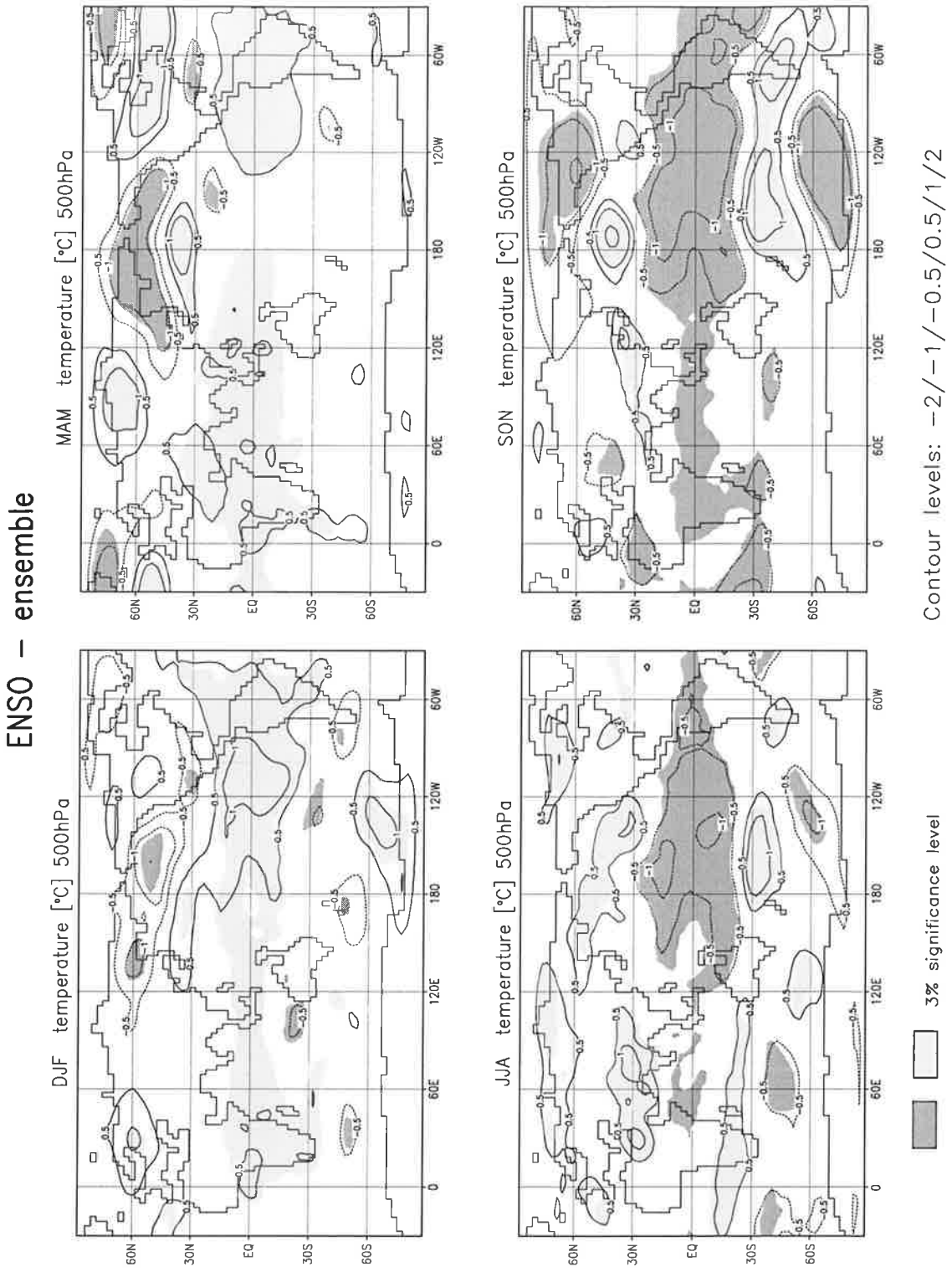

Fig. 9a) Difference of seasonal means of 500 hPa temperature between strong and weak Indian monsoon cases from the ensemble of ENSO-monsoon years. Significance of results at 97% level in a Students´ t-test.

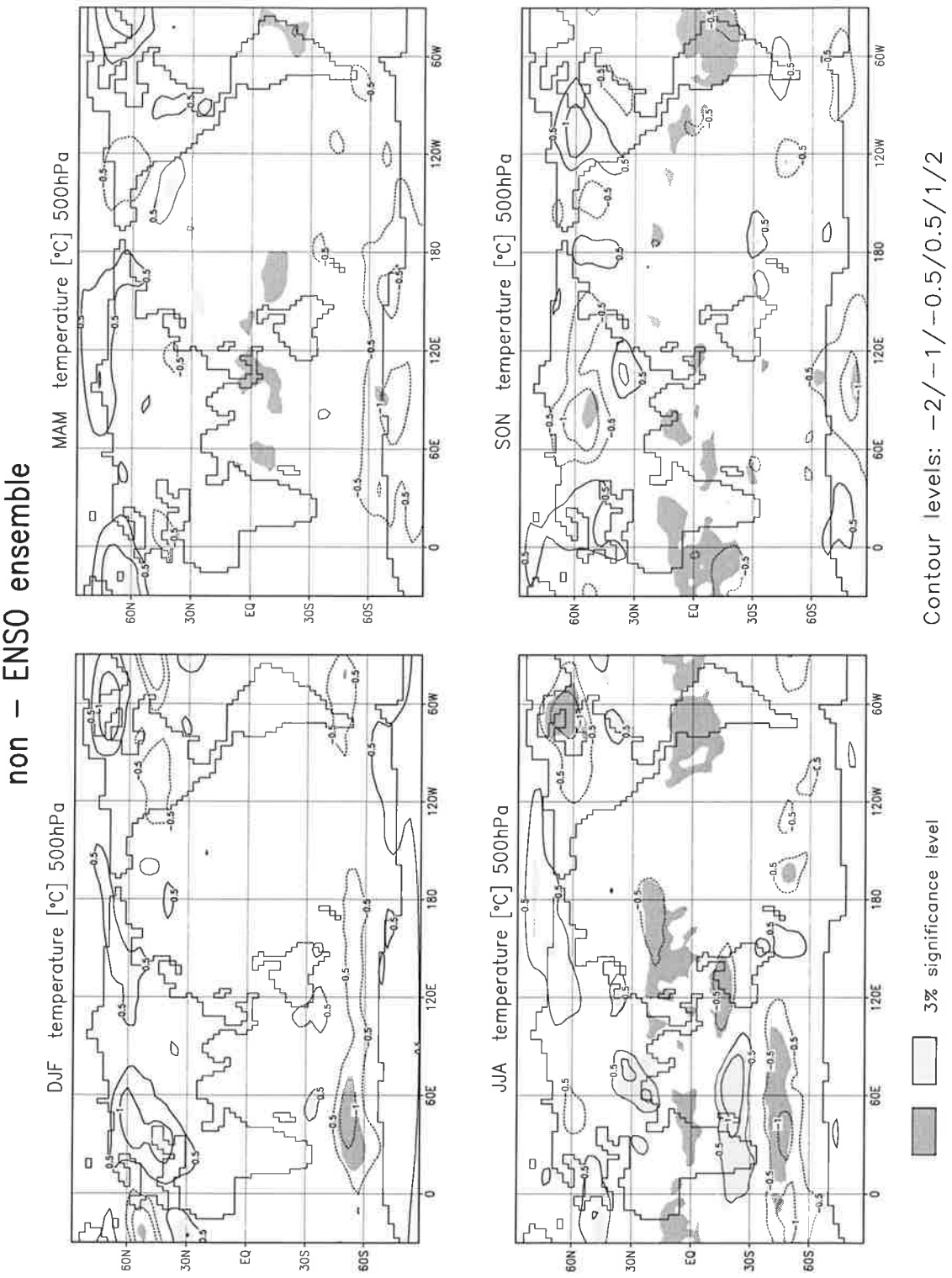

Fig. 9b) As 9a) but for the ensemble of non-ENSO monsoon years.

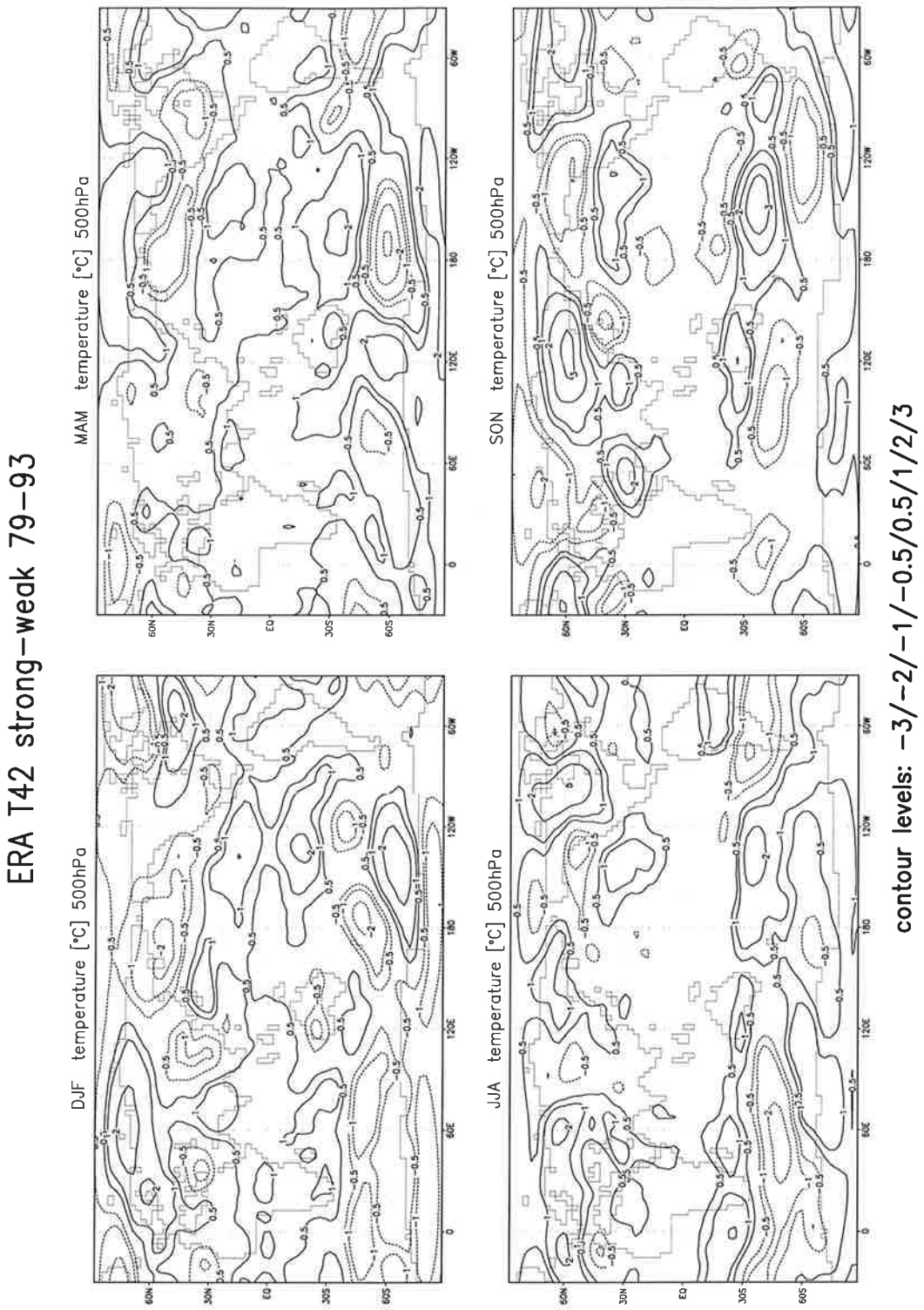

Fig. 9c) Difference of seasonal means of 500 hPa temperature between strong and weak Indian monsoon cases from the ECMWF reanalysis (strong monsoons in 1983 and 1988; weak monsoons in 1982, 1986 and 1987).

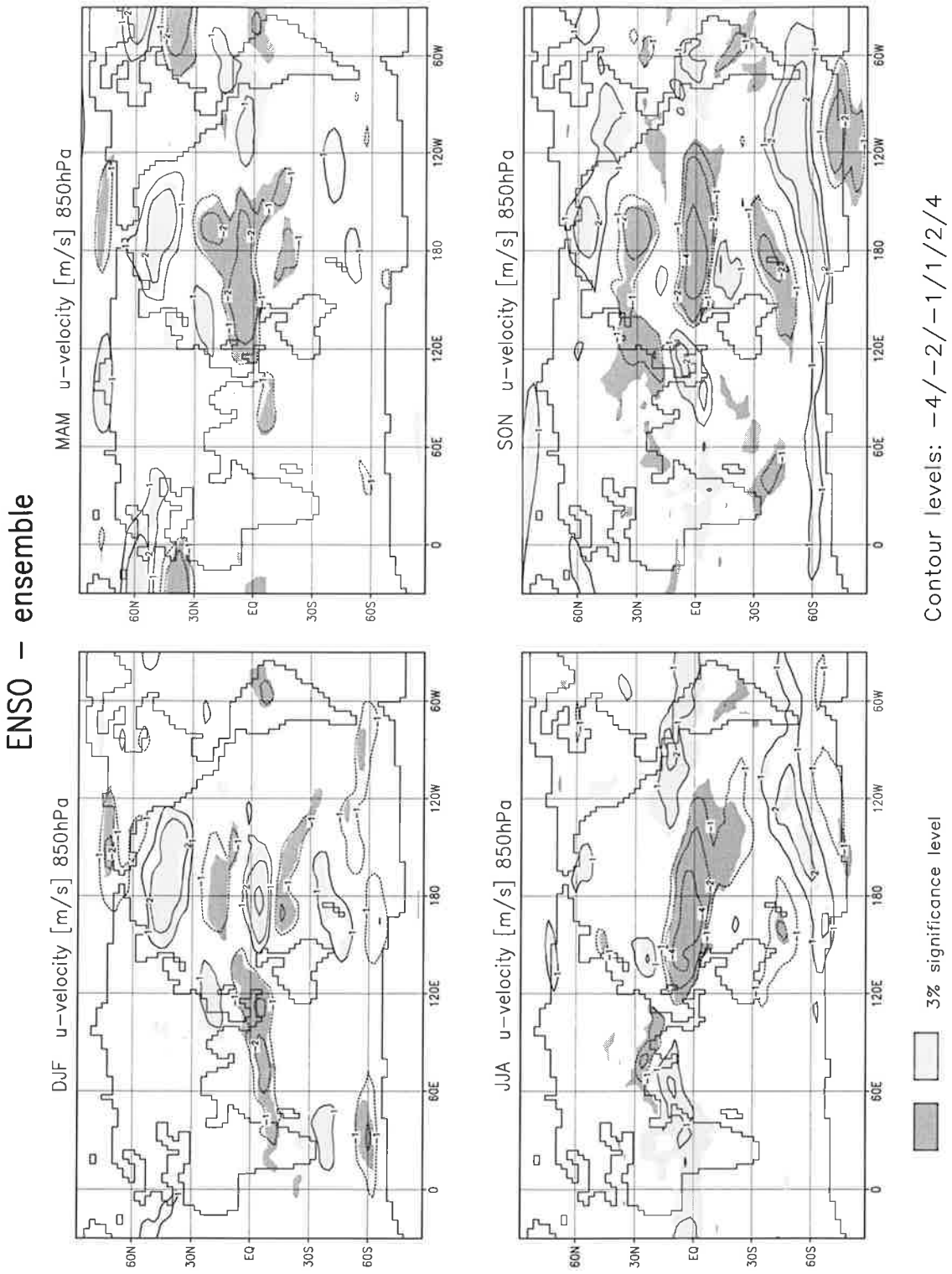

Fig. 10a) Difference of seasonal means of zonal wind velocity at 850 hPa between strong and weak Indian monsoon cases from the ensemble of ENSO-monsoon years. Significance of results at 97% level in a Students´ t-test.

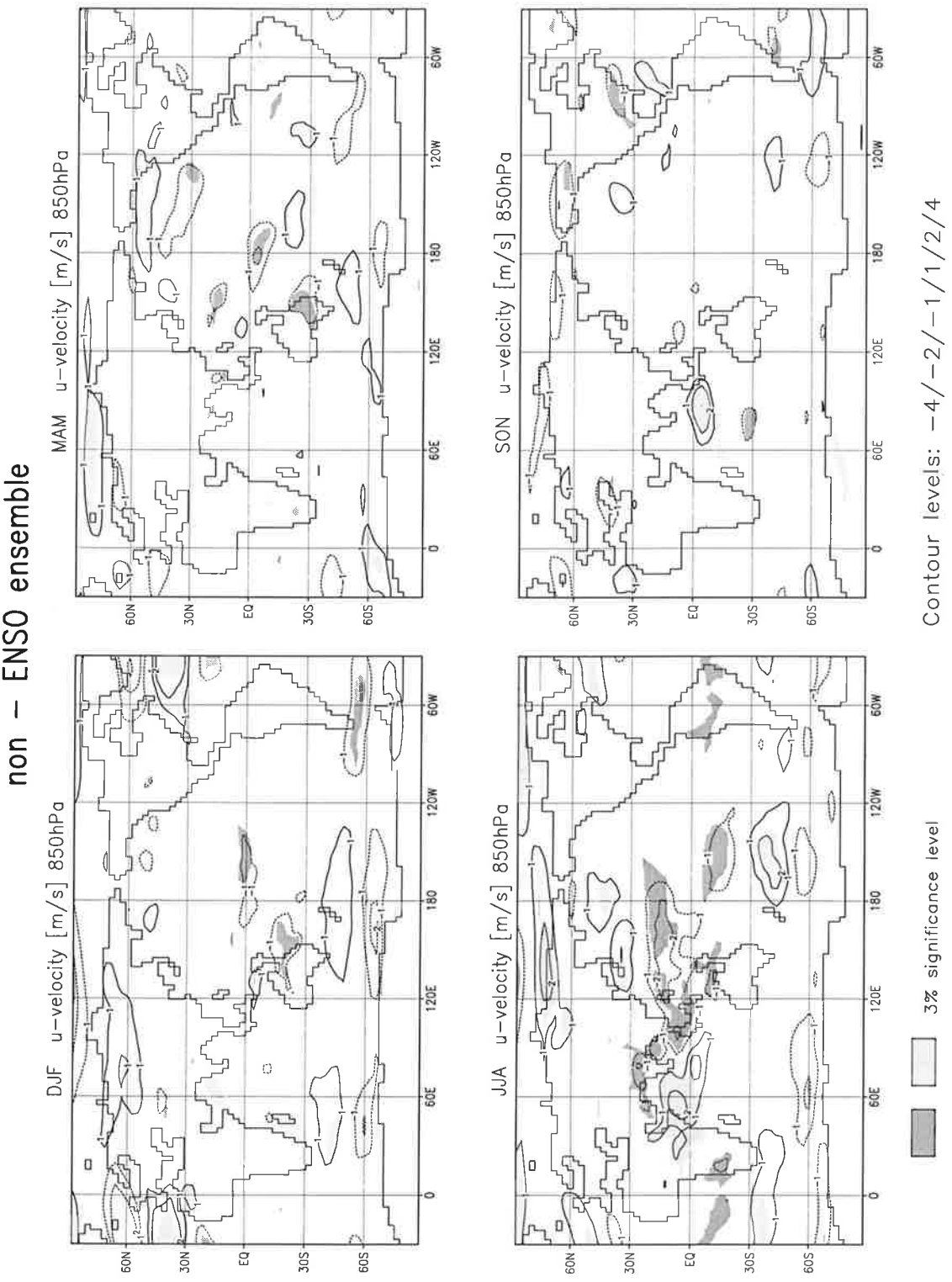

Fig. 10b) As 10a) but for the ensemble of non-ENSO monsoon years.